Drug Design, Development and Therapy

Dovepress
open access to scientific and medical research

Open Access Full Text Article

ORIGINAL RESEARCH

Formulation of Nanospanlastics as a Promising Approach for Improving the Topical Delivery of a Natural Leukotriene Inhibitor (3-Acetyl-11-Keto -β-Boswellic Acid): Statistical Optimization, in vitro Characterization, and ex vivo Permeation Study

This article was published in the following Dove Press journal:
Drug Design, Development and Therapy

Farid Badria[1]
Eman Mazyed[2]

[1]Department of Pharmacognosy, Faculty of Pharmacy, Mansoura University, Mansoura, Egypt; [2]Department of Pharmaceutical Technology, Faculty of Pharmacy, Kafrelsheikh University, Kafrelsheikh, Egypt

Purpose: The current study aimed to discuss the potential of nanospanlastics as a surfactant-based vesicular system for improving the topical delivery of 3-acetyl-11-keto-β-boswellic acid (AKBA). AKBA is a potent anti-inflammatory drug, but it has poor oral bioavailability due to its poor aqueous solubility. Moreover, the topical delivery of AKBA is difficult due to its high lipophilicity. To overcome these drawbacks, AKBA was formulated as deformable elastic nanovesicles and nanospanlastics, for improving its topical delivery.

Materials and Methods: AKBA-loaded spanlastic nanovesicles (SNVs) were formulated by ethanol injection technique according to 2^3 factorial design using Span 60 as a non-ionic surfactant and Tween 80 as edge activator (EA) to investigate the effect of different independent variables on entrapment efficiency (EE%), % drug released after 8 hr (Q_{8h}) and particle size (PS) using Design-Expert software. In vitro characterization, stability test and ex vivo permeation study of the optimized formula were performed.

Results: The choice of the optimized formula was based on the desirability criteria. F7 was selected as the optimized formula because it has the highest desirability value of 0.648. F7 exhibited EE% of 90.04±0.58%, Q_{8h} of 96.87±2.67%, PS of 255.8±2.67 nm, and zeta potential of −49.56 mV. F7 appeared as spherical well-defined vesicles in both scanning electron microscope (SEM) and transmission electron microscope (TEM). The Fourier transform infrared spectroscopy (FTIR) and differential scanning calorimetry (DSC) studies investigated the absence of interaction between AKBA and different excipients and good encapsulation of AKBA within SNVs. F7 retained both physical and chemical stability after storage for 3 months at 4–8 °C. Ex vivo permeation test exhibited significant enhancement of permeability of F7 across rat skin than the free drug.

Conclusion: Nanospanlastics could be a promising approach for improving the permeability and topical delivery of AKBA.

Keywords: AKBA, spanlastics, topical delivery, optimization, edge activator

Correspondence: Eman Mazyed
Department of Pharmaceutical Technology, Faculty of Pharmacy, Kafrelsheikh University, POB 33516, Kafrelsheikh, Egypt
Tel +20 100 3484508
Email eman_mazyad@pharm.kfs.edu.eg

Introduction

Natural products emerge as a valuable and affordable source for potential drugs that may be used as a lead for the treatment of many diseases. *Boswellia* species (family: Burseraceae) is a group of trees found in the Middle East, Northern

submit your manuscript | www.dovepress.com
DovePress
http://doi.org/10.2147/DDDT.S265167

Africa, and India. Frankincense is the oleo-gum resin extruded from the incision of the trunk of several species of *Boswellia*, including *Boswellia serrate* (Indian frankincense) and *Boswellia carterii* (African frankincense). *Boswellia* resin and its components have been used for many therapeutic applications such as anti-inflammatory, hepatoprotective, anti-ulcer, and immunomodulatory effects.[1–6] The main biological active principle of the gum resin is boswellic acids (BAs). BAs inhibit selectively 5-lipoxygenase enzyme which is the key enzyme of leukotriene synthesis that plays a key role in the pathogenesis of inflammation. Among the investigated BAs, 3-Acetyl-11-keto-β-boswellic acid (AKBA) has the strongest inhibitory effect.[7] AKBA is a natural pentacyclic triterpene that has a potent anti-inflammatory effect. Besides, it possesses low toxicity and limited adverse effects compared to other anti-inflammatory drugs due to its direct and non-competitive mechanism on the 5-lipoxygenase enzyme. Unfortunately, its biological applications are limited due to its poor aqueous solubility that decreases its solubility in the intestinal fluids causing poor oral bioavailability. Moreover, AKBA is significantly affected by the hepatic first-pass effect that reduces its systemic absorption.[8] Furthermore, reducing inflammation required a high concentration of AKBA at the site of inflammation. Thus topical delivery of AKBA seems to be a preferred alternative to an oral dosage form, which could be directly applied to the target tissues reducing the frequency of administration and increasing drug efficiency. However, the topical administration of AKBA is difficult due to its high lipophilicity (logP=8).[9]

Several approaches have been utilized to enhance drug permeability across the stratum corneum (SC) in topical drug delivery like conventional colloidal carriers, such as liposomes, niosomes, microemulsions, or solid lipid nanoparticles. However, these carriers have a rigid nature and lack flexibility and deformability during passage through the biological membranes. Therefore, recent studies have been investigated to enhance the elasticity of these conventional carriers to enhance their permeability through different skin layers.[10] Spanlastics are surfactant-based elastic nanovesicles that were developed by Kakkar and Kaur.[11] They consist of a non-ionic surfactant and an edge activator (EA). Recently, there has been a growing interest in using spanlastics for improving the trans-tympanic delivery,[10] the ocular delivery,[12] the trans-ungual delivery[13] and the topical delivery[14] of many drugs. Spanlastics are safe, biodegradable and non-immunogenic vesicular carriers. Besides, they are more chemically stable than liposomes[15] and more advantageous than conventional niosomal dispersions due to their elasticity. The elasticity of spanlastic vesicles is attributed to the presence of EA that acts as a destabilizing factor of the lipid membrane that increases the deformability and permeability of the nanovesicles across biological membranes by enabling them to deform and squeeze through different pores of the skin layers without rupturing.[10] These elastic nanospanlastic vesicles have been used to enhance the topical delivery of many drugs due to improved drug permeation, the capability of controlled delivery of both lipophilic and hydrophilic drugs over a sustained period of time, and hence enhancing the therapeutic efficiency, improving patient compliance and minimizing adverse effects.[14] Inspired by the unique characteristics of spanlastics, this research aims to optimize the topical delivery and the permeability of AKBA through encapsulation into nanospanlastic vesicles.

Materials and Methods

Materials

Silica gel G60F254 for TLC, reversed-phase silica (RP-C18) for column chromatography, silica gel for column chromatography (70–230 mesh) and pre-coated reversed-phase silica plates for TLC were purchased from E. Merck (Darmstadt, Germany), precoated silica gel GF254plates, aluminum and plastic sheets for TLC were obtained from Macherey-Nagel (Düren, Germany). Polyoxyethylene (20) sorbitan monooleate (Tween 80), polyoxyethylene (20) sorbitan monopalmitate (Tween 40), polyoxyethylene (20) sorbitan monolaurate (Tween 20) and cholesterol were obtained from Sigma Chemical Co. (St. Louis, MO, USA). Sorbitan monostearate (Span 60) and sodium lauryl sulfate were purchased from PureLab, USA. Potassium dihydrogen phosphate, potassium monohydrogen phosphate, pentane, diethyl ether, and acetic acid were purchased from Alpha Chemica (Mumbai, India). Absolute ethanol, dimethyl sulfoxide, hydrochloric acid (HCl) and sodium hydroxide (NaOH) were obtained from El-Nasr Pharmaceutical Chemical Company (Cairo, Egypt). Spectra/Pore® cellulose dialysis membranes (Spectra/pore 4, 12,000–14,000 Mwt cut-off) were obtained from Spectrum Laboratories Inc. (Rancho Dominguez, CA, USA). Methanol (HPLC grade), glacial acetic acid (HPLC grade) and methylene chloride were purchased from Sigma-Aldrich Chemical Co. (St. Louis, Missouri,

USA). *Boswellia carterii* Birdwood gum resin was purchased from a local herbal store, Cairo, Egypt. It was authenticated by comparison with genuine samples in the Pharmacognosy Department, Faculty of Pharmacy, Mansoura University. All other chemicals and solvents were of analytical grade and used as received.

Methods

Isolation and Identification of AKBA

Boswellia carterii gum resin (1 kg) was successively extracted using ethanol. The extract was evaporated under vacuum at 45°C using a rotary evaporator (Buchirotavapor R-3000, Switzerland) to obtain a thick brown residue (490.37 g).[16,17] The ethanolic extract was stirred with a 3% NaOH solution (6 L) until the formation of a uniform emulsion. The aqueous part was filtered and extracted with 3 L of hexane/ethyl acetate (95:5 v/v) to remove the non-acidic part. The aqueous portion was then acidified with 1N HCl to precipitate the total organic acids.

The filtered acids were washed several times with distilled water to remove the final traces of HCl. The crude mixture of acids was re-dissolved in 3% NaOH solution and the whole process was repeated until complete precipitation. After washing, the precipitate was dried in a vacuum oven (Binder ED 23-UL) at a temperature below 45°C to yield 279.86 g creamy powder of BAs. For separation of the individual acids, this mixture of BAs was subjected to column chromatography over silica gel (60–120 mesh).

Hexane with increasing proportions of ethyl acetate was eluted through the column for collecting different fractions. Thin-layer chromatography (TLC) was used for monitoring these fractions. TLC was performed on silica gel (pentane/diethyl ether, 2:1 and 1% acetic acid) and simultaneously on RP-18 TLC plates (methanol/water, 19:1).[18]

Similar patterns showing fractions were pooled and evaporated to dryness over a rotavapor under vacuum 45 °C to produce syrupy viscous residues. The residues were then taken in methanol/methylene chloride, purified by different chromatographic methods to finally yield several triterpenoids including AKBA as major acid.[19]

The solubility of AKBA was studied by the equilibrium solubility method using different solvents such as distilled water, Phosphate buffer solution (7.4), Phosphate buffer solution (7.4) and 1% sodium lauryl sulfate (SLS), ethanol and dimethyl sulphoxide (DMSO).[20] The equilibrium solubility method was based on the saturation shake-flask solubility technique. An excess amount of AKBA was added separately to volumetric flasks containing distilled water, phosphate buffer solution (7.4), phosphate buffer solution (7.4) and 1% sodium lauryl sulfate (SLS), ethanol and dimethyl sulphoxide (DMSO). In order to attain the equilibrium condition, the flasks were shaken at 80 rpm over a shaking water bath (Julabo SW 20C, Osaka, Japan) for 72 h at 25°C. 1 mL aliquot was withdrawn, filtered using nylon membrane filter (Nylon Acrodisc, 0.20 mm, Gelman Sciences Inc., USA) and analyzed using HPLC at 260 nm.[21,22]

AKBA was subjected to phytochemical tests such as Liebermann-Burchard test and Salkowski test to investigate its triterpenoidal nature.[23] With respect to the Liebermann-Burchard test, few drops of acetic anhydride were added along with a few drops of concentrated sulphuric acid, from the side of the tube, to chloroformic solution of AKBA (2mL). Salkowski test was performed by shaking a chloroformic solution of AKBA (2mL) with concentrated sulphuric acid (2mL).[24,25]

AKBA was identified using NMR (JEOL-JNM-ECX -400 NMR Spectrometer, Tokyo, Japan). This apparatus was used for the determination of 1H-NMR (Proton Nuclear Magnetic Resonance spectroscopy) and ^{13}C-NMR (Carbon Nuclear Magnetic Resonance spectroscopy). Moreover, mass spectroscopy (JEOLJMS-700 M Station Mass Spectrometer, Tokyo, Japan), melting point determination (Melting point apparatus, Stuart SMP 10) and Fourier transform infrared spectroscopy FTIR (Thermo Scientific™ Nicolet™ iS™10 FTIR Spectrometer) were employed for identifying AKBA.[7,26]

HPLC Assay of AKBA

A validated HPLC procedure was adopted.[27] All chromatographic runs were done using the Dionex UltiMate 3000RS HPLC system (Thermo ScientificTM, DionexTM, Sunnyvale, CA, USA). It consisted of an LPG-3400RS quaternary pump, a TCC-3000RS column thermostat, a WPS-3000RS autosampler, and a DAD-3000RS diode array detector. Chromeleon 7 was the software employed in data collection and processing. Different samples were filtered using nylon membrane filter (Nylon Acrodisc, 0.20 mm, Gelman Sciences Inc., USA) and injected onto an Inertsil reversed-phase C18 (150 × 4.6 mm × 5 µm) column. The mobile phase was acetonitrile-water at a ratio of (90:10, v/v %). The pH of the mobile phase was adjusted using glacial acetic acid to pH 4. The injection volume was 20 µL and the elution was performed at a flow rate of

1.2 mL/min. All assays were done at room temperature.[28] The calibration curve involves plotting peak areas of AKBA against respective standard concentrations of methanolic solutions of AKBA ranging from 10 to 100 µg/mL.[27,29]

Preliminary Screening Studies

Preliminary screening studies were performed to investigate the effect of the addition of EA on the vesicular deformability and to choose the appropriate level of different variables that could improve the elasticity of AKBA-loaded nanospanlastic formulations. For studying the effect of the addition of EA on the elasticity of nanovesicles, three EAs (Tween 80, Tween 40 and Tween 20) were employed for the preparation of three AKBA-loaded nanospanlastic formulations, Table 1 using Span 60 and EA at 90:10 w: w ratio. The conventional AKBA-loaded niosomal formulation was developed, without addition of EAs, using Span 60 and cholesterol at 2:1 w:w ratio to explore the addition of EAs on the elasticity of spanlastics.[30] Different AKBA-loaded nanospanlastics and the conventional niosomal formulation were evaluated for their elasticity. The EA that achieved the best elasticity result was used for further studies.

Selection of the appropriate level of different variables was performed using the selected EA at different Span 60: EA ratios of 90:10, 80:20 and 70:30 at three different speeds of rotation (250, 500 and 1000 rpm) for different sonication times (0, 3 and 5 min). A total of 27 AKBA-loaded nanospanlastic formulations were prepared and evaluated for their elasticity, Table 2.

Preparation of AKBA-Loaded Spanlastic Nanovesicles (SNVs) and the Conventional Niosomes

AKBA-loaded SNVs and the conventional niosomes were prepared by the ethanol injection method.[12,31] Briefly, AKBA (10 mg) together with Span 60 were dissolved into absolute ethanol (2 mL) until a clear solution was attained. The ethanolic solution was injected dropwise using a syringe pump, at a rate of 1 mL/min[32] into preheated (70°C) aqueous phase containing the selected EA that was stirred continuously using a magnetic stirrer (Jenway 1000, Jenway, UK) at 250 rpm. The final volume of the nanospanlastic dispersion was 10 mL. The AKBA-loaded nanospanlastic dispersion was continued to stir for another 1 h for complete evaporation of any remaining ethanol at room temperature. Water-bath ultrasonication (Elmasonic E 30 H, Elma, Singen, Germany) of spanlastic dispersion was performed for 3 min to obtain a suitable vesicle size. The formed AKBA-loaded SNVs were then left to mature overnight at 5°C to be used for further investigation.[31] The same steps were used for preparing the conventional niosomal dispersion without the addition of EA and with the addition of cholesterol to span 60.[30,33]

Measurement of Vesicle Elasticity

The elasticity of nanospanlastic dispersions and the conventional niosomal dispersion was investigated by extrusion through a nylon membrane filter with a 100 nm pore diameter at 2.5 bar for 5 min.[34] The vesicle size of different formulations (before and after filtration) was estimated by a NICOMP 380 ZLS Zeta Potential/Particle Sizer (PSS Nicomp, Santa Barbara, CA, USA). Elasticity was determined in terms of deformability index (DI) using the following equation:

$$DI = J\left(r_v/r_p\right)^2 \quad (1)$$

where J is the amount of the extruded formulation, r_v: the vesicle size of the formulation (after extrusion) and r_p: the pore size of the nylon membrane filter. Statistical significance was evaluated by one-way ANOVA adopting SPSS-11 software (SPSS. Inc., Chicago. IL, USA).

After choosing the most appropriate two levels of each variable that achieved the highest elasticity, 2^3 factorial design would be performed to study the effect of the chosen levels of independent variables on other responses like entrapment efficiency, the percentage of drug released after 8 h and the particle size.

Table 1 Prescreening Study for Investigating the Effect of Addition of EA on Elasticity of AKBA-Loaded SNVs

Formula	Span 60 (mg)	EA (mg)	Cholesterol (mg)	PS Before Extrusion (nm)	PS After Extrusion (nm)	DI
S1	450	50	–	245.8±4.16	239.2±4.24	7.21 ±0.25
S2	450	50	–	265.2±2.53	259.7±1.79	5.91 ±0.16
S3	450	50	–	288.1±3.26	280.5±2.69	4.38 ±0.24
Niosomes	450	–	225	301.5±2.86	40.33±1.72	0.51 ±0.04

Notes: S1; Spanlastic formulation containing Tween 80, S2; spanlastic formulation containing Tween 40, S3; spanlastic formulation containing Tween 20; the values are expressed as mean ± SD; n = 3.

Abbreviations: EA, edge activator; DI, deformability index; PS, particle size.

Table 2 Prescreening Study for the Formulation of AKBA-Loaded SNVs Using Tween 80 as EA

Formula	Ratio of Span 60 to EA	Rotation Speed (rpm)	Sonication Time (min)	DI
P1	90:10	250	0	4.38 ±0.18
P2	80:20	250	0	5.01 ±0.11
P3	70:30	250	0	6.93 ±0.29
P4	90:10	500	0	5.58 ±0.15
P5	80:20	500	0	6.23 ±0.31
P6	70:30	500	0	7.86 ±0.22
P7	90:10	1000	0	6.99 ±0.24
P8	80:20	1000	0	8.24 ±0.36
P9	70:30	1000	0	9.08 ±0.42
P10	90:10	250	3	7.21 ±0.25
P11	80:20	250	3	8.35 ±0.21
P12	70:30	250	3	10.61 ±0.43
P13	90:10	500	3	8.51 ±0.27
P14	80:20	500	3	9.11 ±0.44
P15	70:30	500	3	11.45 ±0.38
P16	90:10	1000	3	9.11 ±0.39
P17	80:20	1000	3	10.36 ±0.42
P18	70:30	1000	3	11.59 ±0.43
P19	90:10	250	5	9.13 ±0.34
P20	80:20	250	5	10.07 ±0.44
P21	70:30	250	5	12.33 ±0.53
P22	90:10	500	5	10.43 ±0.45
P23	80:20	500	5	11.43 ±0.43
P24	70:30	500	5	12.93 ±0.56
P25	90:10	1000	5	11.92 ±0.44
P26	80:20	1000	5	12.21 ±0.41
P27	70:30	1000	5	14.19 ±0.52

Notes: Spanlatic formulations contained Span60 and EA at 90:10 ratio involves using 450 mg Span 60 and 50 mg EA; 80:20 ratio involves using 400 mg Span 60 and 100 mg EA; 70:30 ratio involves using 350 mg Span 60 and 150 mg EA; The values are expressed as mean ± SD; n = 3.
Abbreviations: EA, edge activator; DI, deformability index.

Experimental Design

The factorial design is a statistical approach that is extensively used for planning and optimizing different experimental series.[10] A 2^3 factorial design was established using Design-Expert software, Version 7.0.0 (Stat-Ease, Inc., Minneapolis, Minnesota, USA) to optimize the eight AKBA nanospanlastic formulations and to investigate the relationship between the chosen independent variables and different responses.[14] The ratio of Span 60: EA, speed of rotation and sonication time were considered as the independent variables X1, X2, and X3, respectively. Dependent variables were the entrapment efficiency (EE %, Y1), the percentage of drug released after 8 h (Q_{8h}, Y2) and the particle size (PS, Y3). Each factor was screened at two levels (−1 and +1) that labeled the lower level and the upper level, respectively (Table 3).

The coefficient of determination (R^2), predicted R^2 and adjusted R^2 were used for investigating the goodness of fit of the model to the experimental data.[10] Linearity plots of the observed versus predicted values were also utilized to confirm the validity of the chosen model for different responses.[35] Moreover, the analysis of variance (ANOVA) was used for statistical analysis of the results and determination of the significance level of each term on the basis of F statistics and the P-value.[36]

In vitro Characterization of AKBA-Loaded SNVs

Determination of Drug Content and Entrapment Efficiency of AKBA-Loaded SNVs

Methanol was selected as an appropriate solvent for the disruption of the prepared SNVs for the determination of total drug content.[31] Total drug contents (unentrapped+entrapped) of the prepared formulations were determined by dissolving 0.2 mL of nanospanlastic dispersion in methanol (25 mL) and then measuring drug content using a validated HPLC method at 260 nm.

Table 3 Experimental Runs, Independent Variables and Observed Responses in 2^3 Factorial Design for AKBA-Loaded SNVs

Formula	Variables					
	Independent			Dependent		
	X1	X2	X3	Y1*	Y2*	Y3*
F1	−1	−1	−1	91.23 ±0.82	63.61 ±1.68	245.8 ±1.68
F2	−1	−1	1	74.85 ±1.57	44.09 ±2.74	229.7 ±2.74
F3	−1	1	−1	81.02 ±2.11	65.78 ±1.62	233.7 ±1.62
F4	−1	1	1	62.02 ±1.24	47.71 ±1.64	215.5 ±1.64
F5	1	−1	−1	95.44 ±1.58	95.18 ±2.72	275.7 ±2.72
F6	1	−1	1	80.53 ±2.22	92.05 ±1.55	243.3 ±1.55
F7#	1	1	−1	90.04 ±0.58	96.87 ±2.67	255.8 ±2.67
F8	1	1	1	73.90 ±2.86	93.49 ±1.73	238.4 ±1.73
Independent variables					Low (−1)	High (+1)
X1: Ratio of Span60 to Tween 80					70:30	80:20
X2:Rotation speed (rpm)					500	1000
X3:Sonication time (min)					3	5

Notes: Y1: EE (%), Y2: Q_{8h} (%), Y3: PS (nm), *the values are expressed as mean ± SD; n = 3, #Optimized Formulation.
Abbreviations: EE, entrapment efficiency; Q_{8h}, % drug released after 8h; PS, particle size.

The entrapment efficiency percent (EE %) of AKBA-loaded SNVs was estimated by the indirect method using ultracentrifugation to separate the un-entrapped drug. Samples of 1 mL of AKBA-loaded SNVs were centrifuged at 15,000 rpm for 1 h at 4°C using a cooling centrifuge (HermleLabortechnik GmbH, Germany). The supernatant was separated and filtered using nylon membrane filter (Nylon Acrodisc, 0.20 mm, Gelman Sciences Inc., USA). The concentration of free AKBA was measured by HPLC at 260 nm. Encapsulation efficiency was calculated as follows:[10]

$$EE(\%) = (A1 - A2)x100/A1 \quad (2)$$

where A1 = Initial amount of drug and A2 = Amount of free drug in the supernatant

In vitro Release Study of AKBA-Loaded SNVs

The in vitro release profile of AKBA-loaded SNVs was established using modified Franz diffusion cells. Firstly, hydration of the semi-permeable cellulose membrane was performed for 24 h using a phosphate buffer solution (pH=7.4) at 25°C. The presoaked cellulose membrane was precisely mounted between donor and receptor chambers. Spanlastic dispersions containing entrapped drug equivalent to 1mg of AKBA were placed over the cellulose membrane in the donor compartment. The receptor medium was 20 mL phosphate buffer solution (pH=7.4) and 1% SLS. The phosphate buffer solution was chosen for maintenance of the physiological conditions.[37] 1%SLS was added to maintain sink conditions.

The rotation was adjusted at 50 rpm and the temperature of the medium was kept at 37±0.5 °C. 0.2 mL aliquots were withdrawn at different time intervals and replaced immediately by the same volume of fresh buffer to ensure keeping a constant volume of the receptor medium.[14] Triplicate experiments were performed. Samples were filtered using nylon membrane filter (Nylon Acrodisc, 0.20 mm, Gelman Sciences Inc., USA) and analyzed using HPLC at 260 nm. The results are expressed as mean values ± SD and the release profiles of the spanlastic formulations were plotted by taking the % AKBA released as the Y-axis and time as the X-axis.

For the determination of the appropriate kinetic model and the mechanism of the in vitro release of AKBA from the fabricated nanospanlastics, the data of drug release were analyzed using different mathematical models, including zero-order, first-order, the Higuchi diffusion model, the Korsmeyer- Pappas and the Hixson Crowell equation. The highest coefficient of determination value (R^2) referred to the order of drug release.[38]

Determination of the Particle Size (PS) of AKBA-Loaded SNVs

The determination of PS and polydispersity index (PDI) was performed for investigating the colloidal characteristics of the AKBA-loaded nanospanlastic formulations. The PDI is used to investigate the degree of homogeneity of the vesicle size. The nanospanlastic dispersion (0.1 mL) was suitably diluted by deionized water (10mL). The estimation of vesicle size and PDI was performed using a NICOMP 380 ZLS Zeta Potential/Particle Sizer (PSS Nicomp, Santa Barbara, CA, USA) at 25°C with a scattering angle of 90°.[13,31]

Statistical Optimization of AKBA-Loaded SNVs

Desirability values were determined to choose the optimized formula.[39] The desirability value lies between 0 and 1 and it describes the closeness of different responses to their ideal values. Desirability value close to 1 indicates that the formulation has the most desirable responses and it is selected as the optimized formula. The optimized formula was selected on the basis of maximum EE%, maximum Q_{8h}, and minimum PS. The optimized AKBA-loaded nanospanlastic formula was subjected to further characterization studies.

Characterization of the Optimized AKBA-Loaded SNVs

Scanning Electron Microscopy (SEM)

The optimized AKBA-loaded nanospanlastic dispersion was observed under a scanning electron microscope (JSM 6100 JEOL, Tokyo, Japan). The optimized nanospanlastic dispersion (0.1 mL) was diluted by deionized water (10mL). One drop of the diluted nanospanlastic dispersion was mounted onto the SEM sample aluminum stub using double-sided sticking carbon tape and dried under vacuum. The sample was subsequently coated with gold film. After coating, the SNVs were examined and photographed by SEM.[40]

Transmission Electron Microscopy (TEM)

The optimized nanospanlastic dispersion (0.1 mL) was diluted by deionized water (10mL). One drop of the diluted nanospanlastic dispersion was dropped on a carbon-coated copper grid and left to adhere to the carbon substrate. Phosphotungstic acid (1% w/v) was

added as a negative stain. The overflowed solution was sipped up and dried in the air.[41] After drying, the SNVs were examined and photographed by TEM (JEOL, JEM-1230, Japan).

Determination of Particle Size and Zeta Potential

The optimized AKBA-loaded nanospanlastic dispersion (0.1 mL) was suitably diluted by double distilled water (10mL). Then, the particle size and zeta potential were determined using a NICOMP 380 ZLS zeta potential/particle sizer (PSS Nicomp, Santa Barbara, CA, USA) at 25° C with a scattering angle of 90°. Zeta potential was estimated by observing the electrophoretic mobility of the colloidal nanospanlastic vesicles within an electrical field. Different measurements were performed in triplicate.[13,42]

Fourier Transform Infrared Spectroscopy (FTIR)

Fourier transform infrared spectroscopy was performed using the FTIR spectrometer (FT-IR Shimadzu 8300 Japan). Samples of AKBA, Span 60, Tween80, plain spanlastic vesicles, and the chosen nanospanlastic formula were used. All these samples (3 mg) were mixed with potassium bromide and compressed to form KBr pellets in a hydraulic press (Kimaya Engineers, Maharastra, India). The scanning range was 4000–400 cm^{-1}.[38]

Differential Scanning Calorimetry (DSC) Study

DSC study was carried out using a Shimadzu DSC 60 (Japan, Kyoto). Samples (3 mg) of AKBA, Span 60, Tween80, plain spanlastic vesicles, and the chosen nanospanlastic formula were placed in aluminum pans and sealed. Thermograms were obtained by heating the samples from 20 to 260°C with a scan rate of 10°C/ min.[38]

Effect of Storage on the Stability of the Optimized AKBA-Loaded SNVs

To study the effect of storage on optimized AKBA-loaded nanospanlastic formula, it was stored into a tightly closed glass vial and kept refrigerated (4–8 °C) for three months. The optimized AKBA-loaded nanospanlastic formula was evaluated with respect to its appearance, residual drug content, EE%, and in vitro release profile.[31] The statistical significance was determined by Student's *t*-test using SPSS-11 software (SPSS. Inc., Chicago. IL, USA) where $p \leq$ describes significant difference between the fresh and the stored formulations.

The in vitro release profile of the optimized AKBA-loaded nanospanlastic formula was compared to that of the freshly prepared one according to the similarity factor test[38] described by of Moore and Flanner.[43] The release profiles are said to be similar if the value of f_2 lies between 50 and 100. f_2 is determined according to the equation given below:

$$F2 = 50.\log\left\{\left[1 + \frac{1}{n}\sum_{t=1}^{n}(Rt - Tt)^2\right]^{-0.5}\right\}100 \qquad (4)$$

Where R_t and T_t are the mean % AKBA released from freshly prepared formula and from the stored formula at time t and n is the number of sampling points.

Ex vivo Permeation Studies

Ex vivo permeation study was performed using rat abdominal skin. Prior to performing this experiment, the study protocol was approved by the ethical committee of the Faculty of Pharmacy, Kafrelsheikh University, Egypt (Approval number KFS-2018/12). Male Wistar rats (200 g) were obtained from the National Research Center (Dokki, Giza, Egypt) and placed in a pathogen-free environment in sawdust bed cages. Animal rooms were kept at 25 ± 2 ° C with a relative humidity of 50% and 12 h of light/dark cycle. Prior to the experiments, the rats were adapted in the animal house for at least two weeks under standard conditions.[38] The experimental procedure was done according to the recommendations of the ARRIVE guidelines,[44] the UK Animals (Scientific Procedures) Act, 1986 (ASPA)[45] European Union Directive as 2010/63/EU.[46]

Following sacrificing rats under anesthesia, the abdominal skin hair was carefully removed by shaving without damaging the skin. The skin integrity was verified by photomicroscopic examination under a light microscope (Coslabs micro, India). The skin was excised and the subcutaneous tissue was carefully removed, and the dermal side was wiped using isopropyl alcohol to remove any adhering fats. The rat skin was then washed with saline and soaked in phosphate buffer solution (pH = 7.4) for 2 h before the experiment.

The ex vivo permeation profile of the optimized AKBA-loaded SNVs was conducted and compared to the aqueous dispersion of AKBA. The ex vivo permeation study was performed using modified Franz diffusion cells with a diffusion surface area of 1.76 cm^2. The receptor medium was 20 mL phosphate buffer solution (pH 7.4)

and 1% SLS that maintained at 37°C±0.5°C and stirred at 50 rpm. The abdominal rat skin was fixed so that the SC side faced the donor compartment. The tested formulation (either the optimized spanlastic dispersion or AKBA aqueous dispersion equivalent to 1mg of AKBA) was loaded on the donor compartment. 0.2mL sample was withdrawn at different time intervals and replaced immediately by the same amount of fresh buffer solution.[9] Aliquots were filtered using nylon membrane filter (Nylon Acrodisc, 0.20 mm, Gelman Sciences Inc., USA) and analyzed using HPLC at 260 nm. The experiment was done in triplicate and the results were described as mean ± SD. The statistical significance was determined by Student's *t*-test using SPSS-11 software (SPSS. Inc., Chicago. IL, USA).

The graphs were plotted by comparing the cumulative amount permeated per unit area (μg cm^{-2}) through rat skin as the Y-axis with respect to time as the X-axis. Samples were analyzed using HPLC at 260 nm. The obtained results of the permeation profile were analyzed and evaluated kinetically by different models; zero-order, first-order, the Higuchi diffusion model, the Korsmeyer-Pappas and the Hixson Crowell equation.

To predict the mechanism of permeation of AKBA through rat skin, different permeation parameters were calculated. At steady-state conditions, the drug flux becomes constant and the curve approaches a straight line. The permeation rate of AKBA (flux, J_{ss}) at steady-state was calculated from the slope of the linear portion of the graphical plot of cumulative drug permeated per unit area, for the time period of 6–8 h, versus time. Lag time (t_{lag}) is the time needed to achieve a stable diffusion flow[47] and was estimated from the X–intercept of the linear portion of the permeation plot.[48] Permeability coefficient (Kp) was also calculated by dividing the flux on the initial concentration of AKBA.[14]

Statistical Analysis

Statistical analysis was conducted using SPSS-11 software (SPSS. Inc., Chicago. IL, USA). Statistically significant differences were determined using the Student's *t*-test and ANOVA. Analysis of the results obtained from the eight formulations suggested by the 2^3 factorial design was done using ANOVA by Design-Expert software, Version 7.0.0 (Stat-Ease, Inc., Minneapolis, Minnesota, USA) to determine the influence of the chosen variables on EE%, Q8h and PS. Data were presented as the mean ± SD. The differences were considered statistically significant when $p<0.05$.

Results and Discussion

Isolation and Identification of AKBA

Bioassay-guided fractionation of *Boswellia carterii* oleo-gum resin was performed and resulted in the isolation and characterization of one fatty acid (palmitic acid) and 8 triterpenoids with different skeletons (lupane, ursane, oleanane, and tirucallane) as previously reported by Badria et al.[6] These triterpenoids are lupeol, *β*-boswellic acid, 11-keto- *β* -boswellic acid, acetyl *β* -boswellic acid, acetyl 11-keto- *β* -boswellic acid, acetyl-α-boswellic acid, 3-oxo-tirucallic acid, and 3-hydroxy-tirucallic acid. The TLC screening of the oleo-gum resin and the results of column chromatographic separation of the oleo-gum resin were summarized in Tables S1 and S2, respectively.

AKBA was isolated as colorless needles with m.p of 274±1.92°C. The solubility AKBA was assessed in different solvents (Table S3). AKBA was found to be soluble in ethanol and DMSO. AKBA is poorly soluble in distilled water and aqueous buffer. AKBA solubility in distilled water and the aqueous buffer was 0.023 and 0.038 mg/mL, respectively. The solubility of AKBA increased in the aqueous buffer after the addition of 1% SLS to 0.169 mg/mL.

AKBA responded to the general chemical tests for unsaturated sterols and/or triterpenes giving red-violet ring turning to green color with Liebermann-Burchard test and pink-red color with Salkowski test. These color reactions reflected its triterpenoidal nature.

The IR Spectrum of AKBA showed characteristic peaks at 3437 cm^{-1} (OH stretching), 2930 cm^{-1} (C-H stretching), 1735 cm^{-1} (C = O stretching of aryl acid), 1456 cm^{-1} (C-H bend), 1383 cm-1 (COO− symmetric stretching of carboxylates), 1241 cm^{-1} (C-CO-C) stretching of aryl ketone and 1025cm^{-1} and 988cm^{-1} (ring structures of cyclohexane).[6,9] The ^{1}H-NMR (400 MHz, $CDCl_3$) and ^{13}C-NMR (100 MHz, $CDCl_3$) signals of AKBA were summarized in Table S4 and Figures 1 and 2. Electron ionization-mass spectroscopy (EI-MS) of AKBA, Figure 3 showed a molecular ion peak m/z $[M]^+$= 512 indicating a molecular weight of 512.35 confirming the molecular formula of $C_{32}H_{48}O_5$.

The above results confirmed the chemical structure of AKBA and were in reasonable agreement with previous data reported by Badria et al.[6] The chemical structure of

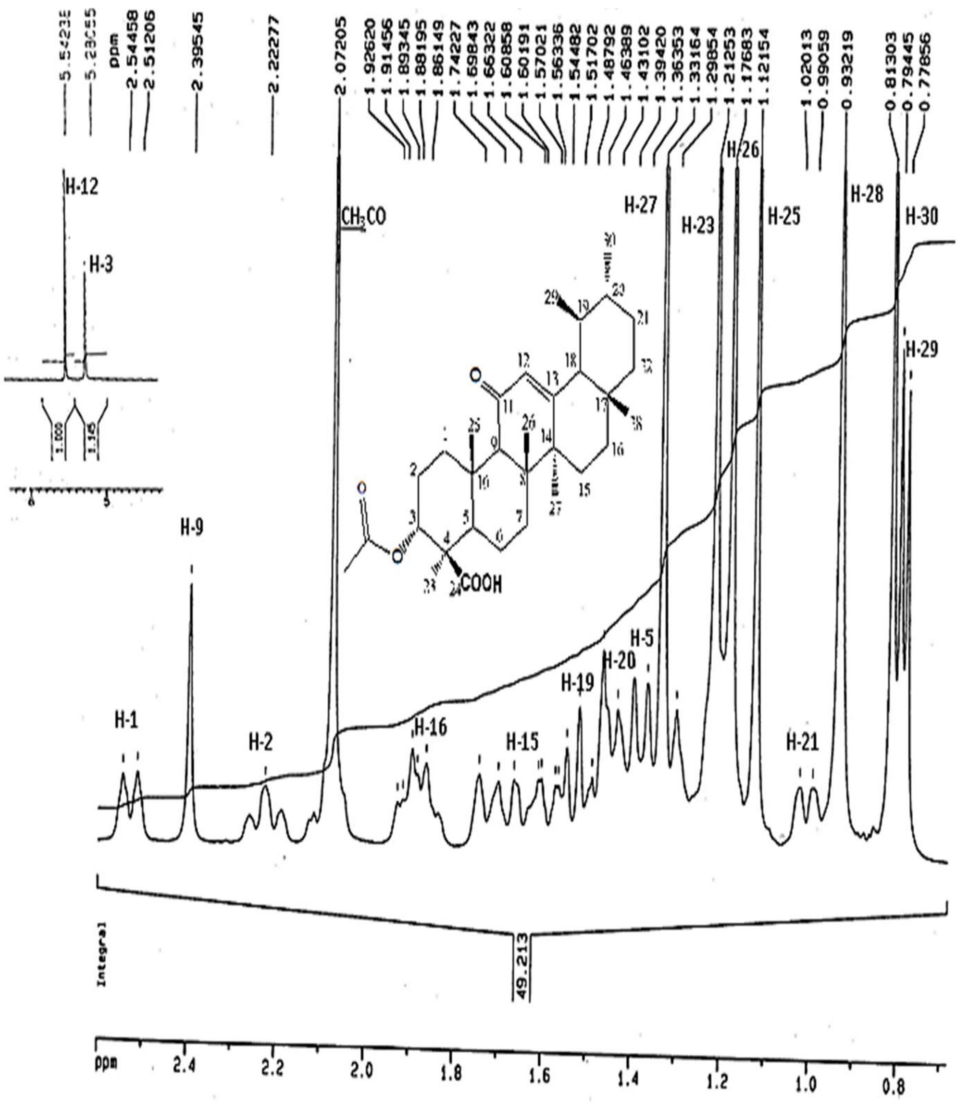

Figure 1 ^{1}H-NMR spectrum of AKBA.
Abbreviations: ^{1}H-NMR, proton nuclear magnetic resonance; AKBA, 3-acetyl-11-keto-β-boswellic acid.

AKBA and other major bioactive triterpenoids isolated from *Boswellia carterii* oleo-gum resin was presented in Figure 4.

HPLC Assay of AKBA

A validated HPLC method was used for the determination of AKBA concentrations within AKBA-loaded SNVs, Figure S1. Effluents were detected at 260 nm. The calibration curve of AKBA was plotted and exhibited a good correlation coefficient value of 0.998. No interfering peaks were noticed in AKBA chromatograms, showing that other components within the spanlastic formulations cause no interference with the estimation of AKBA. The retention time of AKBA was 5.1 min. That is in agreement with data reported by Miscioscia et al.[29] Additionally, Shah et al[27] reported that this technique provided a precise and a rapid method for analyzing boswellic acids from its marketed preparations and performing the quality control tests in the pharmaceutical industry. This method is considered to be a simple and accurate technique for analysis of AKBA. In addition, this method is economical due to its low retention time that decreased both the run time of HPLC analysis and solvent consumption.

Preliminary Screening Studies

The topical carrier delivery system should be deformable so that it could pass through the minute pores of different skin layers and undergo spontaneous deformation to avoid the risk of the vesicular structure rupture.[14] Preliminary

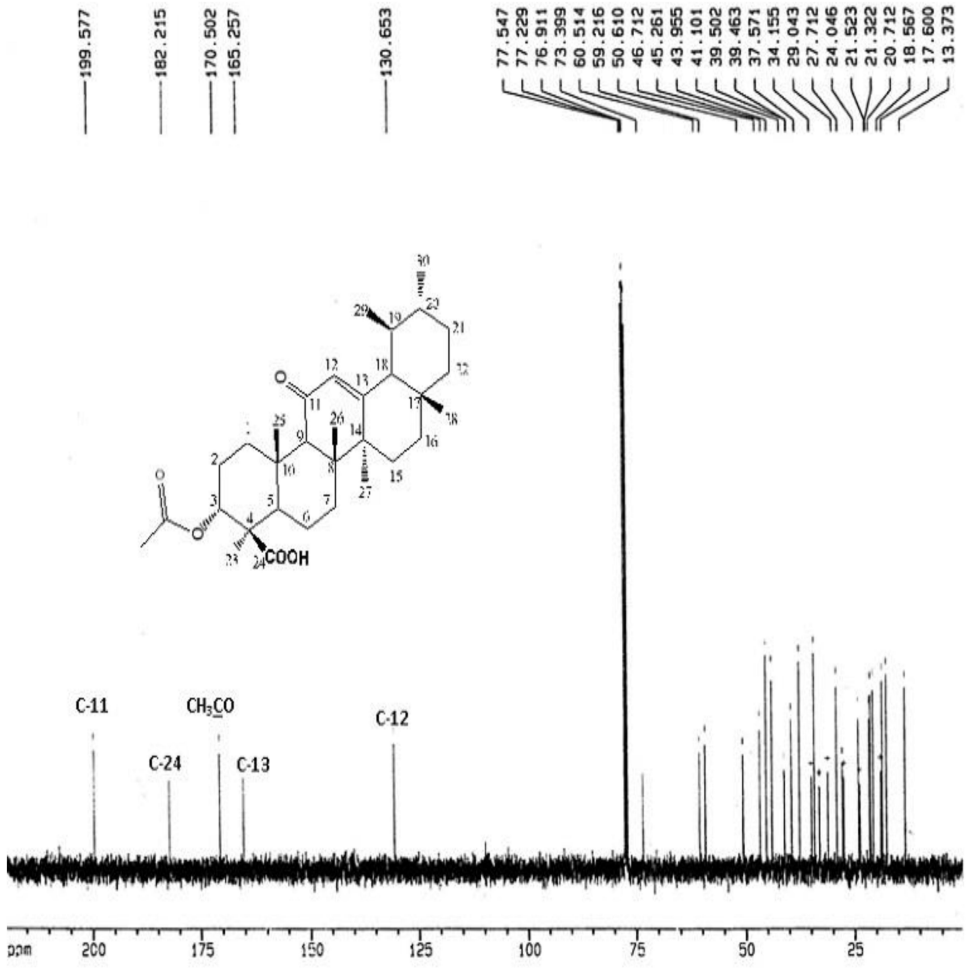

Figure 2 ^{13}C-NMR spectrum of AKBA.
Abbreviations: ^{13}C-NMR, carbon-13 nuclear magnetic resonance; AKBA, 3-acetyl-11-keto-β-boswellic acid.

screening studies were done to inspect the effect of the addition of EA on the vesicular deformability by comparing the elasticity of AKBA-loaded SNVs with a conventional niosomal formulation. In addition, they are used to select the appropriate level of different independent variables that could improve the elasticity of AKBA-loaded SNVs.

Preparation of AKBA-Loaded Spanlastic Nanovesicles (SNVs) and the Conventional Niosomes

AKBA-loaded SNVs and the conventional niosomal dispersion were successfully formulated by the ethanol injection method. Some researchers prepared spanlastics using the ethanol injection method such as Fahmy et al,[31] Basha et al[12] and Elsherif et al.[13] However, others including Al-Mahallawi et al[10] and Farghaly et al[14] used the thin film hydration technique. The ethanol injection method was chosen due to its simplicity, reproducibility, and possibility to obtain small nanovesicles with narrow distribution simply by injecting the ethanolic lipid solution into water (one step–based method).[49] Spanlastics are formulated using a non-ionic surfactant and EA. In the present study, Span 60 was selected as the non-ionic surfactant. The lipophilic and saturated alkyl chain of Span 60 facilitates the development of stable unilamellar and/or multi-lamellar vesicles with high encapsulation efficiency.[31]

Measurement of Vesicle Elasticity

The effect of the addition of EA on the elasticity and deformability of spanlastics was explored by comparing their elasticity with a conventional niosomal formulation that has no EAs. The elasticity of different AKBA-loaded SNVs and the conventional niosomal dispersion was expressed in terms of DI, Table 1. It was observed that the DI of AKBA-loaded SNVs was significantly (p<0.001)

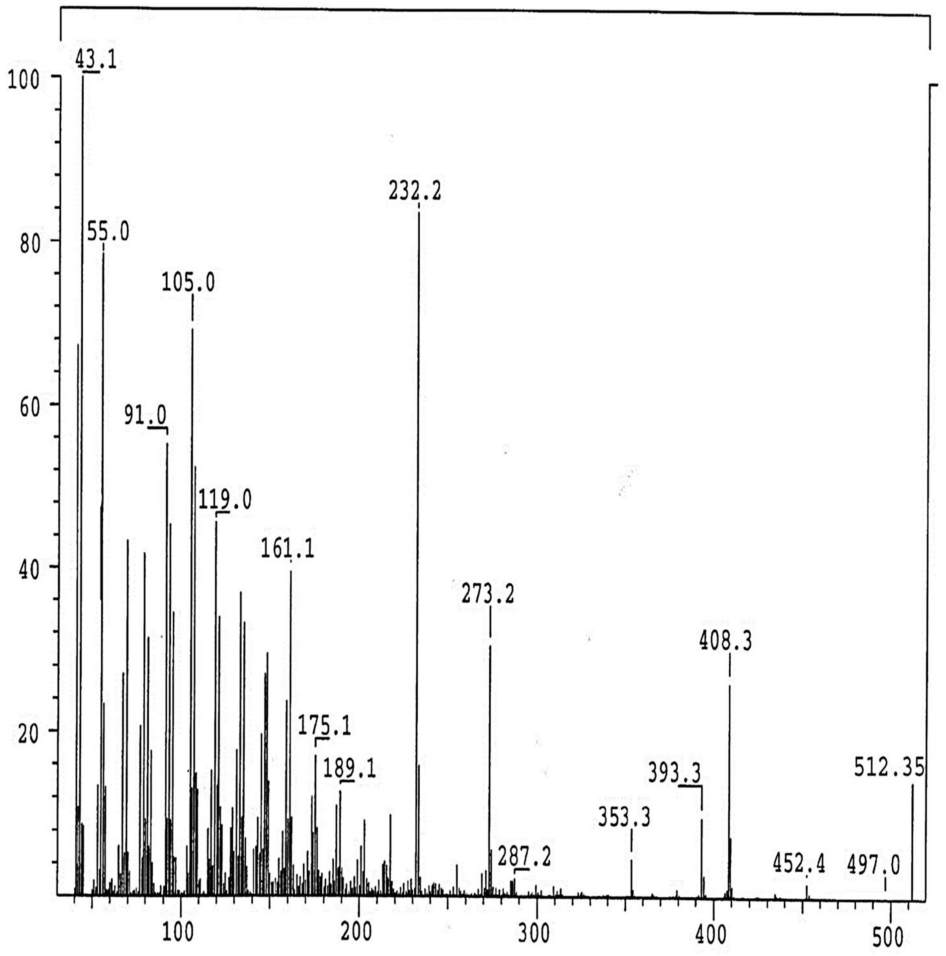

Figure 3 EI/MS fragmentation pattern of AKBA.
Abbreviations: EI/MS, electron ionization/mass spectrometer; AKBA, 3-acetyl-11-keto-β-boswellic acid.

higher than that of the conventional niosomal vesicles. The vesicle size of the nanovesicles was compared before and after extrusion. No significant difference ($p>0.05$) was detected in the size of AKBA-loaded SNVs before and after extrusion. These results investigate the elasticity and flexibility of the spanlastic dispersion and their ability to retain their vesicular size after extrusion. However, the vesicle size of the niosomal dispersion decreased significantly ($p<0.001$) after extrusion that may be due to the rupture of vesicles during passage through the membrane showing that they are non-elastic.[50] These results are in agreement with Manosroi et al[33] who reported that the deformability index of the elastic niosomes was higher than that of the conventional niosomes. This difference between SNVs and the conventional niosomes is attributable to the addition of EA that destabilizes the lipid bilayer improving its elasticity and deformability and enhance the ability of nanovesicles to squeeze through different biological membranes without losing their integrity.[51]

Besides, the preliminary screening study was used to choose the EA that could achieve the highest elasticity for AKBA-loaded SNVs. It was detected that the elasticity of Tween 80 nanospanlastic vesicles was higher than other EAs (Tween 40 and Tween 20). That could be attributed to the flexible and non- bulky hydrocarbon chains of Tween 80 and the presence of unsaturated alkyl chain (double bond) that render the nanospanlastic dispersion prepared using Tween 80 more deformable.[52] Therefore, Tween 80 was the chosen EA that was used for further pre-screening study.

The second part of the preliminary study involved selecting the appropriate level of different independent variables by evaluation of the elasticity of different AKBA-loaded nanospanlastics using Tween 80 as the EA at different Span 60: Tween 80 ratios of 90:10, 80:20 and 70:30 at

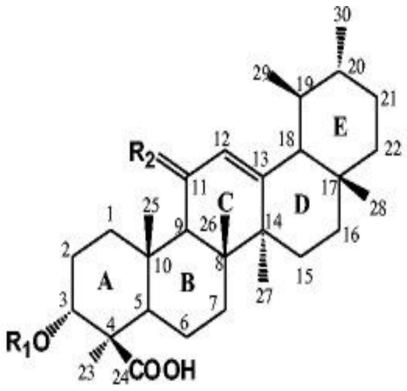

R1	R2
Ac	2 H: *acetyl-β-boswellic acid*
Ac	O: *acetyl-11-keto-β-boswellic acid (AKBA)*
H	2 H: *β-boswellic acid*
H	O: *11-keto-β-boswellic acid*

Figure 4 The chemical structure of AKBA and other major bioactive triterpenoids isolated from *Boswellia carterii* oleo-gum resin.
Abbreviation: AKBA, 3-acetyl-11-keto-β-boswellic acid.

three different speeds of rotation (250, 500 and 1000 rpm) for different sonication times (0, 3 and 5 min), Table 2. DI of different AKBA-loaded nanospanlastics was in the range of 4.38 ±0.18 to 14.19 ±0.52. Concerning the ratio of Span 60: EA, it was found that DI increased as the ratio of Span 60: EA decreased. That may be due to higher concentrations of EA that increased the deformability of the lipid bilayer.[53] In addition, DI increased as rotation speed and sonication time increased. That could be explained on the basis of decreasing vesicle size meaning that more vesicles could pass through small pores of the membrane.[13,54]

According to the preliminary screening trials, Tween 80 was selected as the EA. In addition, the ratio of Span 60: Tween 80, speed of rotation and sonication time were further screened using 2^3 factorial design at two selected levels; (80:20, 70:30), (500, 1000 rpm) and (3, 5 min), respectively.

Analysis of Factorial Design

The factorial design is a very useful tool in the development and optimization of new drug delivery systems due to its ability to analyze the effect of various variables on the properties of formulations.[55] Table 3 shows the composition and the measured responses (EE%, Q_{8h}, and PS) of AKBA nanospanlastic formulations prepared according to the 2^3 factorial design. Table S5 and Figures 5–7 elucidated the relationship between the independent variables and different responses.

Regression equations (Table S5) were established using Design-Expert Software in terms of coded factors. These equations could be used for the identification of the relative effect of different factors by comparing the factor coefficients. The negative sign in front of the factor coefficients indicated that factor had a negative influence on different dependent variables. While the positive sign for the factor coefficients showed a positive effect on different dependent variables.[35]

The predicted R^2 values were estimated for measuring the response value predictability of this model. The adjusted and the predicted R^2 values should be within about 0.20 of each other to be in acceptable agreement.[10] Table S5 shows that the predicted R^2 values of different responses were in a reasonable agreement with the adjusted R^2. Moreover, adequate precision determines the signal to noise ratio and it indicates that the model can be used for navigating the design space. In the present model, adequate precision was found to be more than 4 (the desired value) in all responses.

Data of different responses (Y1, Y2, and Y3) provided a good and significant fit to the linear model (R^2=0.9768, 0.9644 and 0.9615 respectively). Since the values of R^2, predicted R^2 and adjusted R^2 are relatively high for different responses, the obtained equations are highly statistically valid and form an excellent fit to the obtained data.

The predicted and the observed responses of AKBA-loaded nanospanlastics were compared to confirm the validity of this model. Figure 5 demonstrates a good correlation between the experimental and the predicted values of different responses (Y1, Y2, and Y3).

ANOVA analysis (Table S6) was used for estimation of the significance of different factors. *P*-value <0.05 indicates that the model terms are significant because F values are above the critical F values and thus make the *p*-values lower than the threshold level (0.05). Therefore, the null hypothesis H_0 is rejected and the alternative hypothesis is accepted.

The main effects model was used for the representation of the studied responses because it was significant and adequately fitted the data. The 2^3 factorial design was employed to study the effect of the independent variables on different responses as follows:

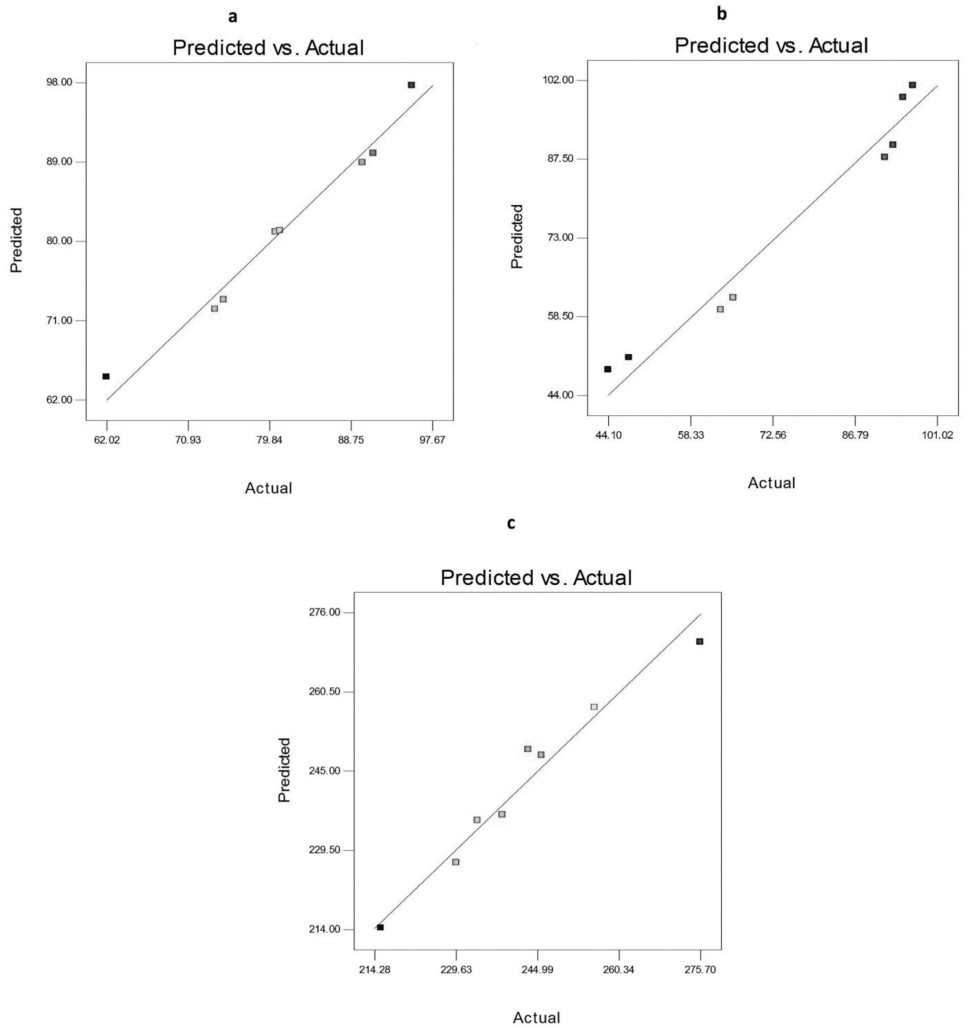

Figure 5 Linearity plots of AKBA-loaded SNVs shown as observed versus predicted values of (**A**) EE%, (**B**) Q_{8h}, and (**C**) PS.
Abbreviations: EE, entrapment efficiency; Q_{8h}, % drug released after 8h; PS, particle size.

The Effect of Formulation Variables on EE% of AKBA-Loaded SNVs

The EE% is an important tool for measuring both drug retention and nanovesicles stability.[56] AKBA-loaded SNVs exhibited good entrapment efficiency that ranged from 62.02±1.24 to 95.44±1.58, Table 3.

ANOVA analysis (Table S6) showed that the ratio of Span 60: Tween 80 (X1), rotation speed (X2) and sonication time (X3) significantly affected the EE% of the prepared nanospanlastics. The effect of different independent variables on the EE% of AKBA-loaded SNVs is shown in Figure 6.

Concerning the effect of the ratio of Span 60: Tween 80 (X1) on EE%, it was clear that X1 has a significant positive effect ($p<0.05$) on drug entrapment in the nanovesicles. That may be attributed to reduced fluidization of the vesicular membrane that leads to decreasing the leakage of the encapsulated drug and hence, increased the EE%.[10] These results were shared by Chauhan and Malik[57] who investigated the synergistic influence of the ratio of Span: EA on EE% of vancomycin hydrochloride-loaded spanlastics.

With respect to rotation speed (X2), it was clear that rotation speed had a significant negative effect on EE% ($p<0.05$) that may be due to decreasing the size of the nanospanlastic vesicles by increasing the speed of rotation.[54]

In addition, sonication time (X3) had a significant negative effect ($p<0.001$) on EE% of AKBA in the prepared nanospanlastic vesicles. Exposing the prepared nanospanlastic vesicles to sonication for 5 min resulted in a significant reduction in EE%. That may be attributable to decreasing the particle size of the nanovesicles. In addition, during disrupting and re-aggregation of

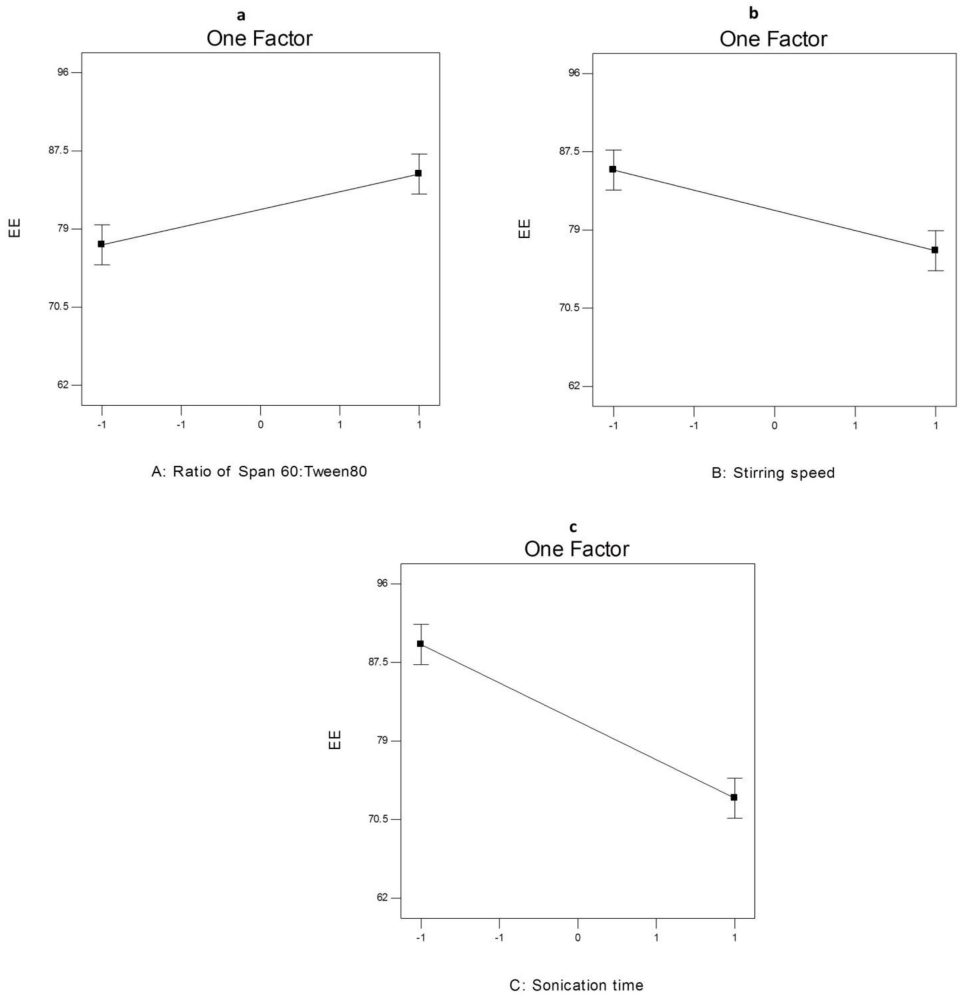

Figure 6 The effect of different independent variables (**A**) ratio of Span 60 to Tween 80, (**B**) stirring speed and (**C**) sonication time on EE% of AKBA-loaded SNVs.
Abbreviations: EE, entrapment efficiency; AKBA, 3-acetyl-11-keto-β-boswellic acid; SNVs, spanlastic nanovesicles.

vesicles, the drug may escape to the external aqueous environment containing surfactant and remain within the aqueous phase by micellar solubilization rather than entrapment in the nanospanlastic vesicles.[58,59] These results agreed with data reported by Elsherif et al[13] in their study about the formulation of nanospanlastics for trans-ungual delivery of Terbinafine Hydrochloride. They found that increasing the time of sonication resulted in a reduction of the size of the nanovesicles with a concomitant decrease in EE%. These findings were also shared by Andersen et al[60] in their study about chitosomes and pectosomes of metronidazole. They concluded that increasing the time of sonication resulted in decreasing the %EE due to the reduction of PS.

The drug content of the prepared AKBA-loaded SNVs (entrapped + un-entrapped) was found to be in the range of 86.24±1.54 to 102.18±1.82.

The Effect of Formulation Variables on Q_{8h} from AKBA-Loaded SNVs

Figure 7 shows the results of the in vitro release of AKBA from different nanospanlastic vesicles. Q_{8h} varied from 44.09±2.74% to 96.87±2.67% (Table 3). F7 achieved the highest % drug released. It is clear that the prepared nanospanlastic formulations exhibited controlled drug release pattern that could be attributed to the release of entrapped drug from the nanovesicles by squeezing through the membrane pores.[14]

The effect of different independent variables on Q_{8h} of AKBA from nano- spanlastic vesicles is shown in Figure 8. ANOVA analysis (Table S6) revealed that both the ratio of Span 60: Tween 80 (X1) and sonication time (X3) have a significant impact on Q_{8h}. However, rotation speed (X2) has no significant effect on Q_{8h} ($p>0.05$).

The ratio of Span 60: Tween 80 (X1) exhibited a significant positive impact on Q_{8h} of the prepared

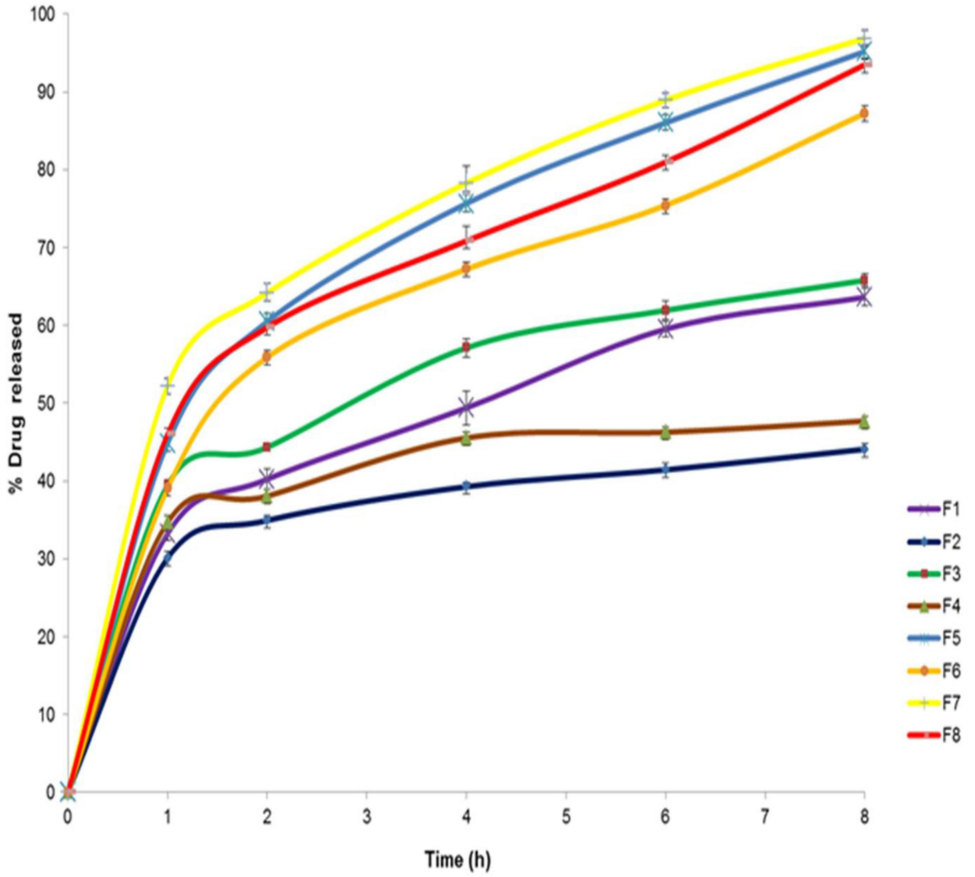

Figure 7 The in vitro release profile of AKBA-loaded SNVs, (n = 3).
Abbreviations: AKBA, 3-acetyl-11-keto-β-boswellic acid; SNVs, spanlastic nanovesicles.

nanospanlastics (p<0.001). These results are in accordance to El Zaafarany et al[61] who reported that drug release decreased upon increasing the amount of EA, due to the formation of mixed micelles that were less sensitive to concentration gradient than the vesicles. Moreover, Jain et al[62] investigated that increasing the surfactant concentrations could result in loss of the vesicular structures and development of mixed micelles.

In addition, it was noted that sonication time (X3) had a significant negative effect on drug release from the nanovesicles (p<0.05). Usually, smaller vesicles release a higher amount of drug than larger vesicles due to increasing their surface area and decreasing the diffusional distance traveled by the drug.[63] However, in the present study, the %AKBA released from SNVs decreased by increasing the sonication time. That could be explained on the basis of agglomeration of spanlastic vesicles due to increasing the free energy of the spanlastic dispersion after excessive sonication that results in a thermodynamically unstable system.[64] This finding was also shared by Elsherif et al[13] in their in vitro release study of the nanospanlastics of Terbinafine Hydrochloride. In this study, increasing the sonication time to 5 min had an inversely proportional influence on the %drug released from Terbinafine Hydrochloride -loaded spanlastics. The kinetic analysis (Table 4) exhibited that the release of AKBA from the fabricated nanospanlastic vesicles fitted best with Higuchi's diffusion model that showed the highest R^2 values.

The Effect of Formulation Variables on PS of AKBA-Loaded SNVs

Table 3 shows that different AKBA-loaded SNVs were in the nano-scale range because their PS ranged between 215.5±1.64 nm and 275.7±2.72 nm. ANOVA results (Table S6) revealed that the ratio of Span 60: Tween 80 (X1), rotation speed (X2) and sonication time (X3) significantly affected the PS of the prepared nanospanlastics (p < 0.05) for all variables.

Figure 9 illustrates the effect of different independent variables on the PS of the AKBA-loaded SNVs. Concerning the ratio of Span 60: Tween 80 (X1), it was

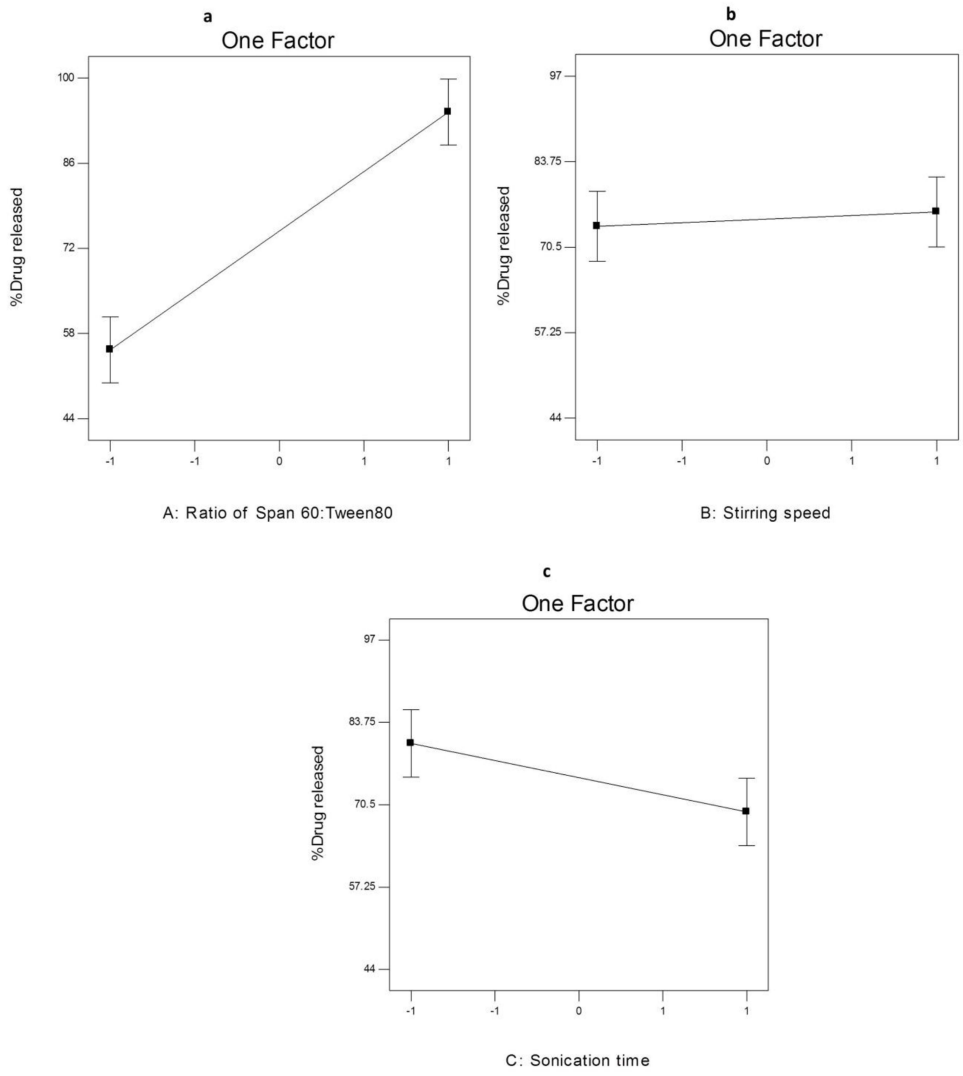

Figure 8 The effect of different independent variables (**A**) ratio of Span 60 to Tween 80, (**B**) stirring speed and (**C**) sonication time on Q_{8h} of AKBA-loaded SNVs.
Abbreviations: Q_{8h}, % drug released after 8h; AKBA, 3-acetyl-11-keto-β-boswellic acid.

obvious that the PS of the formulated nanovesicles decreased upon increasing the concentration of EA (Tween 80) that may be attributable to the reduction of interfacial tension that facilitates particle partition and formation of smaller nanovesicles.[65] Moreover, the small PS could be due to the formation of mixed micelles that have a smaller diameter than the vesicles.[12]

Regarding the effect of rotation speed (X2), it is clear that the PS of the formulated nanovesicles was adversely affected by rotation speed. These results are in accordance to data reported by other researchers as Yassin et al[54] who reported that the PS of the formulated nanospanlastics decreased by increasing the speed of rotation due to the formation of a thin and uniform lipid layer that resulted in producing small spherical vesicles upon hydrating the vesicles.

With respect to sonication time (X3), it was observed that sonication of AKBA-loaded nanospanlastic vesicles for 5 min caused a significant decrease in the PS of the vesicles that might be due to exposing the vesicles to ultrasonic radiation for a longer time.[13]

ANOVA test demonstrated that there was a significant difference in PS between the AKBA-loaded spanlastics ($p<0.05$). However, this variation in the PS was not wide. Moreover, the prepared nanospanlastic vesicles exhibited PDI values that ranged from 0.072 to 0.355 with no significant difference in PDI ($p>0.05$) between different nanospanlastic formulations. The size distribution of the AKBA-

Table 4 The Calculated Correlation Coefficients for the in vitro Release of AKBA-Loaded SNVs Employing Different Kinetic Orders

Formula	Zero Order	First Order	Higuchi Model	Hixson Crowell	Korsmeyer- Pappas
F1	0.9872	−0.9944	0.9971	0.9926	0.9957
F2	0.9648	−0.9726	0.9894	0.9700	0.9812
F3	0.9477	−0.9617	0.97468	0.95718	0.96658
F4	0.9255	−0.9311	0.9626	0.9293	0.9364
F5	0.9765	−0.9812	0.9952	0.9946	0.9926
F6	0.9732	−0.9781	0.9897	0.9878	0.9851
F7	0.9842	−0.9793	0.9988	0.9969	0.9953
F8	0.9880	−0.9682	0.9951	0.9866	0.9791

loaded nanospanlastic vesicles was expressed in terms of PDI which is the ratio of standard deviation (SD) to mean PS. The values of PDI that approach zero showed high homogeneity of the dispersion.[10] Some researchers such as Danaei et al reported that the acceptable PDI range for drug delivery using nano-carriers is 0.3 and below because it indicates the homogenous population of nano-vesicles.[66] These findings investigated the homogenous distribution of the AKBA-loaded nanospanlastic formulations[67] and the reproducibility of the method of preparation.[68]

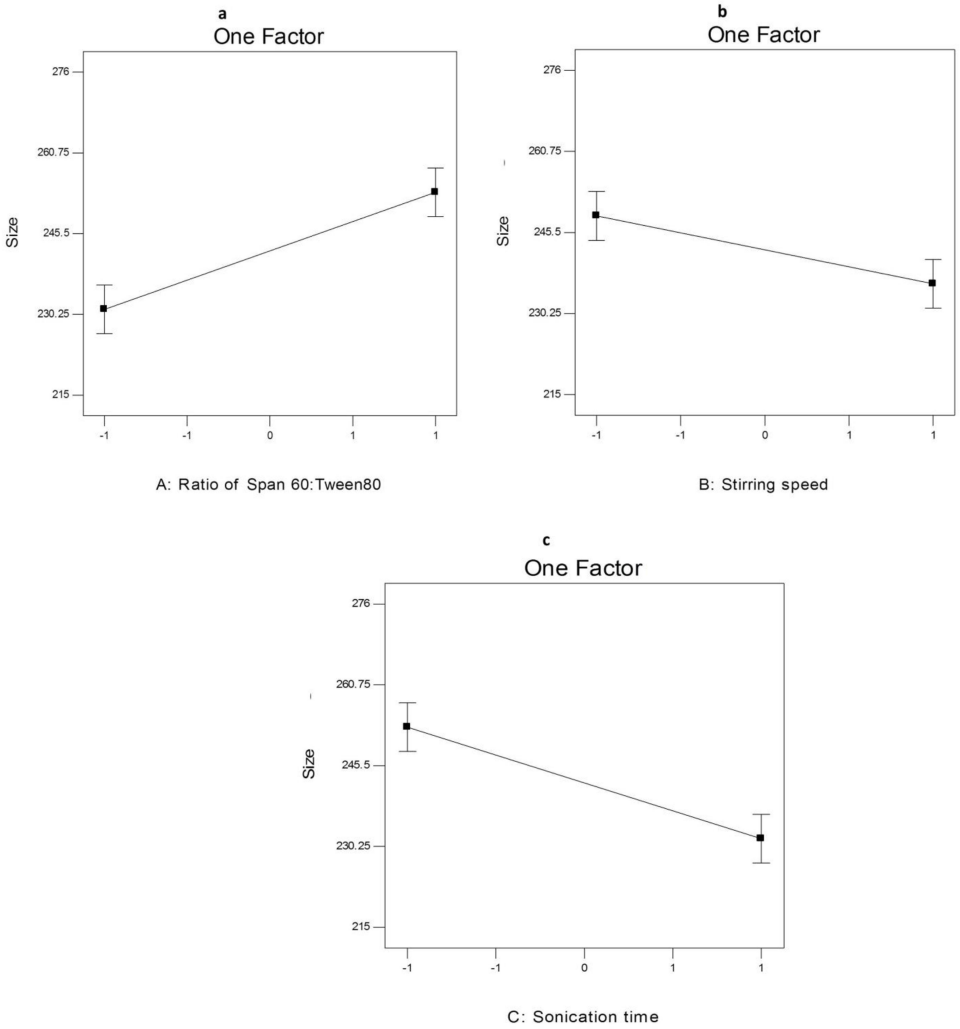

Figure 9 The effect of different independent variables (**A**) ratio of Span 60 to Tween 80, (**B**) stirring speed and (**C**) sonication time on PS of AKBA-loaded SNVs.
Abbreviations: PS, particle size; AKBA, 3-acetyl-11-keto-β-boswellic acid.

Optimization of AKBA-Loaded Nanospanlastics

The optimum values of different variables were determined through numerical optimization using the Design-Expert software program for selecting the optimized AKBA nanospanlastic formula.[69] The choice of the optimized nanospanlastic formula was based on the desirability criteria. Different formulations were optimized for the EE% (Y1), Q_{8h} (Y2), and PS (Y3). The aim was to maximize EE% and Q_{8h} and minimize PS. Results showed that F7 had the highest desirability value of 0.648. Hence, F7 could be considered as the optimized formula and a promising nanospanlastic formula that was chosen for further studies. The optimized formula (F7) was formulated using Span 60 as a non-ionic surfactant and Tween 80 as an EA at the weight ratio of 8:2 using ethanol injection method at a speed of rotation 1000 rpm for 3 min sonication time.

Characterization of the Optimized AKBA-Loaded SNVs

Morphological Characterization by SEM

The SEM micrograph of the optimized AKBA loaded nanospanlastic formula (Figure 10A) revealed that the nanospanlastic vesicles are homogenous, well-identified and of a nearly perfect spherical shape with sharp boundaries. That may be attributed to the formation of closed bilayer vesicles in water due to the amphoteric nature of the non-ionic surfactants that results in the orientation of the hydrophobic portion away from the aqueous environment, whereas the hydrophilic portion remains in contact with the aqueous environment.[70] In addition, the spherical shape of AKBA- loaded SNVs could be due to their tendency to reduce their surface free energy.[38,71]

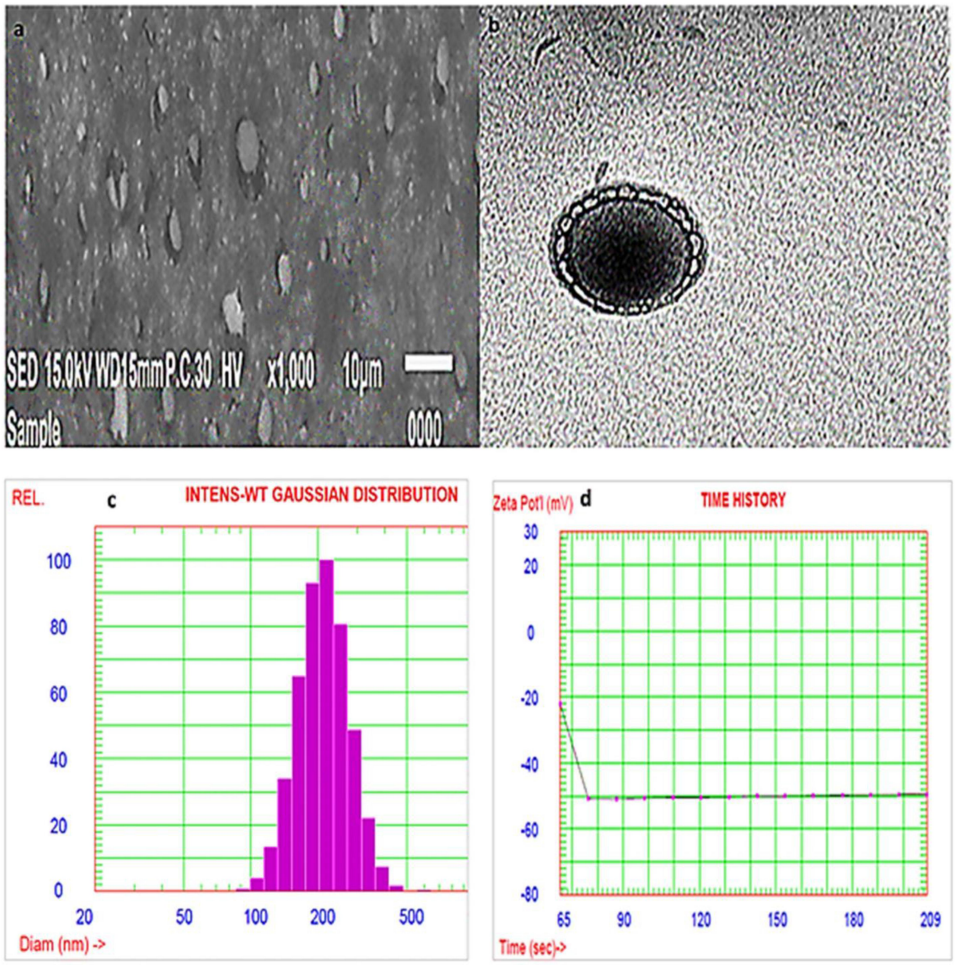

Figure 10 Scanning electron micrograph (**A**), transmission electron micrograph (**B**), particle size distribution curve (**C**) and zeta potential (**D**) of the optimized AKBA-loaded SNVs.

Morphological Characterization by TEM

Transition electron micrographs confirmed the results of SEM (Figure 10B). The examined SNVs appeared as spherical unilamellar nanovesicles with sharp boundaries.

Determination of Particle Size and Zeta Potential

The PS of the optimized AKBA-loaded spanlastic formula (F7) was found to be 255.8±2.67 nm, Figure 10C and with a PDI value of 0.135. The stability of colloidal dispersion is described by zeta potential which is a measure of the net charge of the nanovesicles. The colloidal dispersion that has large positive or negative zeta potential is considered to be stable because the high charge on the vesicle surface creates repulsion between the vesicles that makes them stable without agglomeration providing a uniformly distributed suspension.[72] The chosen spanlastic formula has a high negative zeta potential value of −49.56 mv indicating that the chosen formula is stable, (Figure 10D). The high zeta potential value investigates a low agglomeration tendency of the spanlastic vesicles due to the development of a high-energy barrier between these vesicles. These results agreed with Elsherif et al[13] who reported that the colloidal system is considered to be stable when the value of zeta potential is about ±30 mV due to electric repulsion between the nanovesicles.

Fourier Transform Infrared (FTIR) Spectroscopy

The FTIR spectra of AKBA, Tween 80, Span 60, plain (drug-free) spanlastic formula and the optimized spanlastic formula are illustrated in Figure 11. The FTIR spectrum of AKBA was previously discussed.

The IR spectrum of Tween 80 exhibited peaks at 2907 and 2855 cm^{-1} associated with the asymmetric and symmetric stretching vibrations of methylene ($-CH_2$), respectively. The band at 1735 cm^{-1} originates from the C=O stretching of the ester group. The strong band around

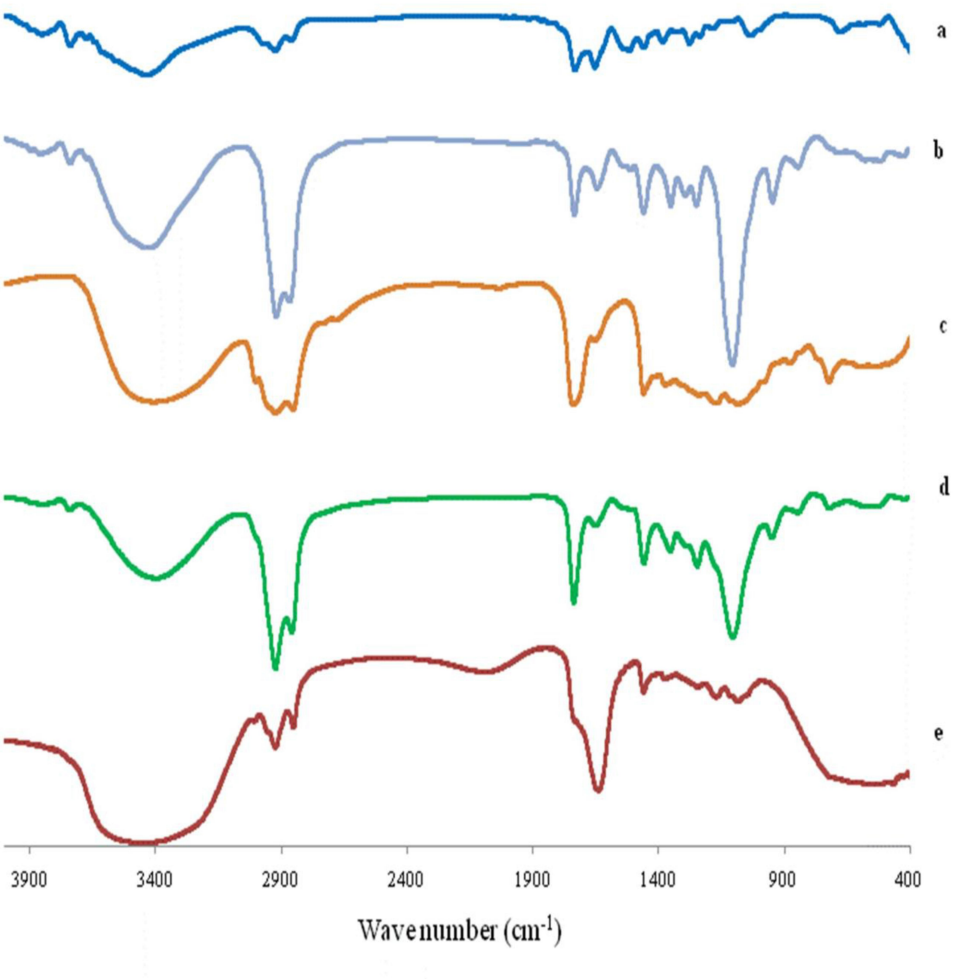

Figure 11 FTIR spectrum of (**A**) AKBA, (**B**) Tween 80, (**C**) Span 60, (**D**) Plain spanlastic and (**E**) the optimized AKBA-loaded SNVs.
Abbreviations: AKBA, 3-acetyl-11-keto-β-boswellic acid; SNVs, spanlastic nanovesicles.

3436 cm^{-1} can be attributed to the O-H stretching vibrations.[73] Span 60 exhibited characteristic peaks at 3410 cm^{-1} which is due to aliphatic O–H stretch, 2936 cm^{-1} (C–H stretch) and 1745 cm^{-1} (C=O stretch of ester).[74]

The FTIR spectrum of the plain (drug-free) spanlastic formula exhibited the characteristic peaks of both Tween 80 and Span 60. Reducing the intensity of the peaks of both Tween 80 and Span 60 in the plain spanlastic formula may be explained on the basis of lipid bilayer formation.[38] These results agreed with El-Sayed et al[74] who reported that the IR spectrum of drug-free niosomes exhibited the characteristic peaks of Span 60 and cholesterol with reduced intensity due to the development of the lipid bilayer structure.

Moreover, the FTIR spectrum of the optimized spanlastic formulations displayed the characteristic peaks of AKBA and different excipients which indicated the absence of interaction between AKBA and different excipients. Minor shifting and reduced intensity of the characteristic peaks of AKBA may be attributable to the formation of hydrogen bonds, Van der Wall forces, or dipole interactions between AKBA and other excipients increasing both the encapsulation of AKBA and the stability of the nano-vesicles.[38] These findings are in accordance with Fathalla et al[75] who reported the absence of interactions between the drug and other ingredients of the Anthralin-loaded ethosomal formulations according to the FTIR spectrum that displayed the characteristic peaks of both drug and excipients with a little shift.

Differential Scanning Calorimetry (DSC) Study

DSC is an important tool for detecting both the physical state and thermal behavior of the drug. DSC thermograms of AKBA, Tween 80, Span 60, plain (drug-free) spanlastics and the optimized spanlastic formula are presented in Figure 12. The DSC thermogram of AKBA depicted an endothermic melting peak at 282.3°C that revealed the crystallinity of AKBA.[76] The DSC thermogram of Tween 80 exhibited an endothermic peak at 113.8°C that

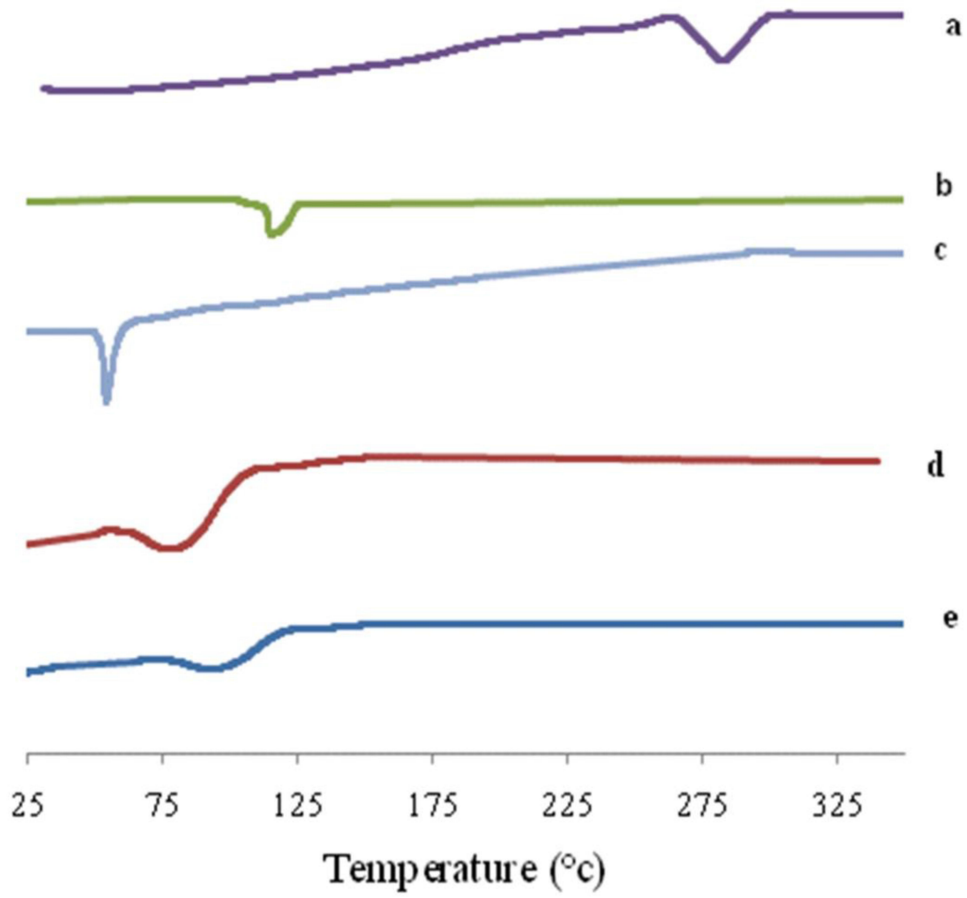

Figure 12 DSC thermogram of (**A**) AKBA, (**B**) Tween 80, (**C**) Span 60, (**D**) Plain spanlastic and (**E**) the optimized AKBA-loaded SNVs.
Abbreviations: AKBA, 3-acetyl-11-keto-β-boswellic acid; SNVs, spanlastic nanovesicles.

corresponds to its flash point.[77,78] Span 60 showed a characteristic endothermic peak at 54.4°C corresponding to its transition temperature.[79] The plain nanospanlastics showed the appearance of a new endothermic peak at 80.2°C that may reflect the interaction of the components of the nanospanlastic vesicles during the formation of the lipid bilayer[74] and the role of Tween 80 in reducing the cooperativity of transition because Tween 80 acts as an EA that disrupts the packing characteristics and, accordingly, fluidizes the lipid bilayer.[80]

The chosen nanospanlastic formula showed a shift of the endothermic peak of the lipid bilayer to 89.9°C and disappearance of the endothermic peak of AKBA that may be attributed to entrapment of AKBA in the nanospanlastic vesicles and dispersion of AKBA as an amorphous state in the nanospanlastic formulation increasing the phase transition temperature of nanospanlastic vesicles. These findings are in reasonable agreement with Mazyed et al[35] who concluded that the complete disappearance of the endothermic peak of acetazolamide, in the DSC thermogram of the transfersomal formulation, could be attributable to the loading of acetazolamide within the transfersomal nanovesicles in the amorphous state.

Effect of Storage on the Stability of the Optimized AKBA-Loaded SNVs

Table 5 investigates the effect of storage for three months at 4–8 °C on the stability of the optimized AKBA-loaded SNVs. It is clear that the optimized SNVs retained both chemical and physical stability. There was no observed change in the appearance of SNVs. Moreover, there was no significant difference in the drug content, EE% and Q_{8h} of the stored formula when compared to the fresh one ($p > 0.05$). In addition, the release profile of the stored formula was compared with the fresh one using the similarity factor test. f_2 was found to be 78 indicating a non-significant difference in drug release from the optimized SNVs after storage. These results are in accordance with Fahmy et al[31] who detected non-significant change between the stored and the fresh haloperidol-loaded spanlastic gels with respect to the appearance, the drug content and the release profiles. They reported that the small difference in the release profiles of the fresh and stored formulations could be attributable to the limited leakage of the drug from nano-spanlastic vesicles but it was non-significant.

Table 5 Effect of Storage on the Properties of the Optimized AKBA-Loaded SNVs (F7)

Parameter	Fresh F7	Stored F7
*Drug content (%)	98.54±0.65	95.94±0.37
*EE (%)	90.04±0.58	86.85±0.44
*Q_{8h} (%)	96.87±0.82	94.65±1.47

Notes: *Each value represents mean ± SD (n = 3). F7: the optimized AKBA-loaded SNVs.
Abbreviations: EE, entrapment efficiency; Q_{8h}, % drug released after 8h; PS, particle size.

Comparative ex vivo Permeation of the Optimized AKBA-Loaded SNVs

For investigating the effect of encapsulation of AKBA in nanospanlastic vesicles on its permeation through the skin, an ex vivo permeation study was performed. Table 6 and Figure 13 demonstrate the results of AKBA permeation from the optimized nanospanlastic formula (F7) in comparison with free AKBA. It was found that AKBA dispersion diffused inefficiently through the rat skin reaching the maximum cumulative amount permeated per unit area of 101.77 ±2.48 µg cm^{-2} after 8 h; whereas the optimized nanospanlastic formula (F7) showed higher permeation through the rat skin reaching 363.50 ±5.86 µg cm^{-2} cumulative amount permeated per unit area after 8 h. Moreover, the ex vivo permeation parameters showed that the optimized nanospanlastic formula had a significant enhancement of AKBA flux across the skin ($p<0.05$) than AKBA dispersion, with an enhancement ratio of 3.34. The enhancement of flux was also associated with a reduction in the t_{lag} compared to free drug. The t_{lag} is the time required to achieve a stable diffusion flow[47] and it describes the diffusion of the drug through the skin.The trend of t_{lag} reduction after application of spanlastic formulation (F7) could be attributed to increased diffusivity of AKBA and skin penetration enhancement.[48]

The enhanced delivery of nanospanlastic vesicles could be interpreted on the basis of higher flexibility and elasticity of nanospanlastic vesicles due to presence of Tween 80 as the EA that acts as a destabilizing factor of the lipid membrane increasing the deformability and permeability

Table 6 Ex vivo Permeation Parameters of the Optimized AKBA-Loaded SNVs and AKBA Dispersion

Formula	*t lag (h)	*Jss (µg cm^{-2} hr^{-1})	*K_P (cm hr^{-1})	ER
AKBA dispersion	0.63 ±0.05	7.84±0.45	0.0078±0.15	–
F7	0.16 ±0.02	26.21±1.53	0.0262±0.12	3.34

Notes: *Each value represents mean ± SD (n = 3). F7: the optimized AKBA-loaded SNVs.
Abbreviations: t_{lag}, lag time; J_{ss}, steady state flux; K_P, permeability coefficient; ER, enhancement ratio.

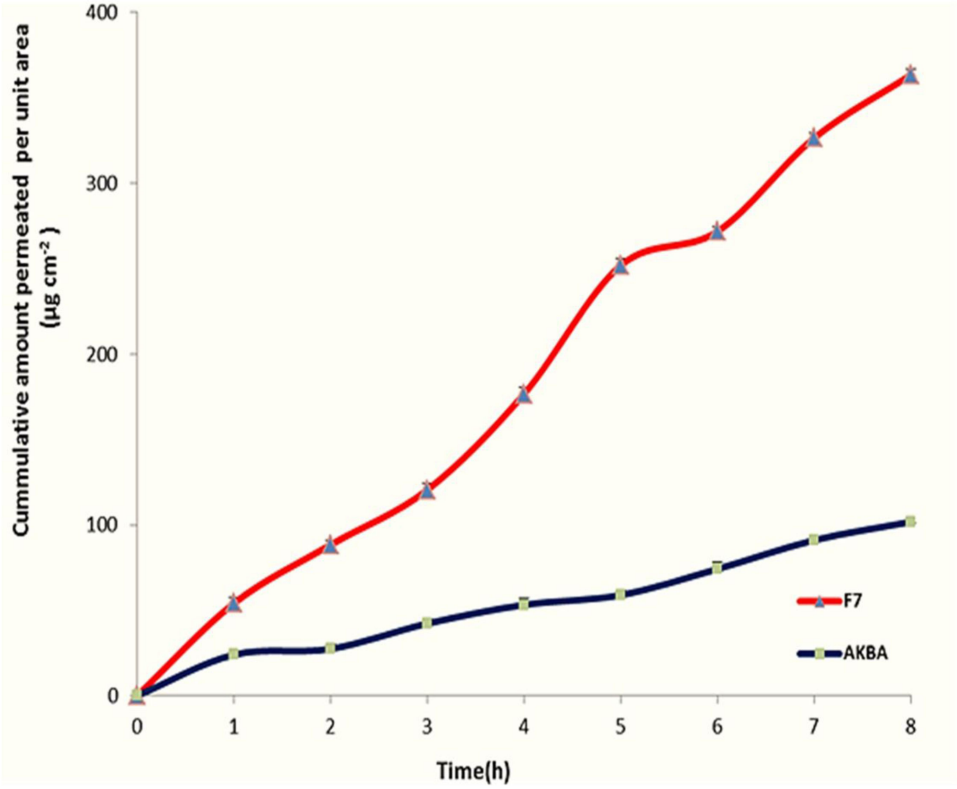

Figure 13 Ex vivo permeation profile through hairless rat skin of AKBA dispersion and the optimized AKBA-loaded SNVs, (n = 3).
Abbreviations: AKBA, 3-acetyl-11-keto-β-boswellic acid; SNVs, spanlastic nanovesicles.

of the nanovesicles across biological membranes by squeezing through different pores of the skin layers without rupturing.[81]

The kinetic analysis of the permeation profile of both AKBA dispersion and the nano- spanlastic formula exhibited that the zero-order model was the best fitting model that had the highest correlation coefficient values (Table 7). That may be explained on the basis of the constant concentration gradient of the drug across the rat skin membrane.[82] Consequently, the flux of both AKBA dispersion and F7 across the membrane would be constant and followed zero-order kinetics, because the flux is a function of the concentration gradient. In such cases, Fick's law could be used to relate fluxes and concentration gradients. Figures S2 and S3 investigates the kinetics graphs of ex vivo permeation of AKBA dispersion and F7, respectively according to zero order.

Conclusions

In the present study, a promising non-ionic surfactant based vesicles, SNVs, were effectively fabricated as nano-sized elastic vesicles by the ethanol injection method using Span 60 and EAs. A 2^3 factorial design was used for the optimization of different nanospanlastic formulations. The optimized nanospanlastic formula (F7) showed spherical morphology, good release profile and relatively high drug entrapment efficiency. The ex vivo permeation studies showed that the encapsulation of AKBA into nanospanlastics had succeeded to increase the drug permeation due to higher deformability and permeability of the SNVs by

Table 7 The Calculated Correlation Coefficients for the ex vivo Permeation of the Optimized AKBA-Loaded SNVs and AKBA Dispersion Employing Different Kinetic Orders

Formula	Zero Order	First Order	Higuchi Model	Hixson Crowell	Korsmeyer- Pappas
AKBA dispersion	0.9918	−0.9898	0.9696	0.9905	0.9580
F7	0.9946	−0.9884	0.9822	0.9920	0.9626

Note: F7: the optimized AKBA-loaded SNVs.

squeezing through narrow pores of the skin layers without rupture. In brief, the obtained findings investigate that the deformable nanospanlastics can be a breakthrough for the enhancement of the topical delivery of AKBA.

Disclosure

The authors declare that they have no conflicts of interest to disclose. Moreover, this research did not receive any specific grant from funding agencies in the public, commercial or not-for-profit sectors.

References

1. Badria FA, El-Farahaty T, Shabana AA, Hawas SA, El-Batoty MF. Boswellia-curcumin preparation for treating knee osteoarthritis: a clinical evaluation. *Altern Complement Ther*. 2002;8(6):341–348. doi:10.1089/107628002761574635
2. Badria FA, Mohammed EA, El-Badrawy MK, El-Desouky M. Natural leukotriene inhibitor from Boswellia: a potential new alternative for treating bronchial asthma. *Altern Complement Ther*. 2004;10(5):257–265. doi:10.1089/act.2004.10.257
3. Badria FA, Houssen WE, El-Nashar EM, Saaed SA. Effect of glycyrrhizin and Boswellia carterii extract on liver injury: biochemical and histopathological evaluation. *Biosci Biotech Res Asia*. 2003;1(2):93–96.
4. Badria FA. Preparation a new product of natural origin for treatment of hyperacidity and colitis. Egyptian Patent; 2001;23376.
5. Yusif RM, Hashim IIA, Mohamed EA, Badria FA-E. Gastroretentive matrix tablets of boswellia oleogum resin: preparation, optimization, in vitro evaluation, and cytoprotective effect on indomethacin-induced gastric ulcer in rabbits. *AAPS PharmSciTech*. 2016;17(2):328–338. doi:10.1208/s12249-015-0351-8
6. Badria FA, Mikhaeil BR, Maatooq GT, Amer MM. Immunomodulatory triterpenoids from the oleogum resin of Boswellia carterii Birdwood. *Zeitschrift für Naturforschung C*. 2003;58(7–8):505–516. doi:10.1515/znc-2003-7-811
7. Mostafa DM, Ammar NM, Basha M, Hussein RA, El Awdan S, Awad G. Transdermal microemulsions of Boswellia carterii Bird: formulation, characterization and in vivo evaluation of anti-inflammatory activity. *Drug Deliv*. 2015;22(6):748–756. doi:10.3109/10717544.2014.898347
8. Mehta M, Dureja H, Garg M. Development and optimization of boswellic acid-loaded proniosomal gel. *Drug Deliv*. 2016;23(8):3072–3081. doi:10.3109/10717544.2016.1149744
9. Goel A, Ahmad FJ, Singh RM, Singh GN. 3-Acetyl-11-keto-β-boswellic acid loaded-polymeric nanomicelles for topical anti-inflammatory and anti-arthritic activity. *J Pharm Pharmacol*. 2010;62(2):273–278. doi:10.1211/jpp.62.02.0016
10. Al-Mahallawi AM, Khowessah OM, Shoukri RA. Enhanced non invasive trans-tympanic delivery of ciprofloxacin through encapsulation into nano-spanlastic vesicles: fabrication, in-vitro characterization, and comparative ex-vivo permeation studies. *Int J Pharm*. 2017;522(1–2):157–164. doi:10.1016/j.ijpharm.2017.03.005
11. Kakkar S, Kaur IP. Spanlastics—a novel nanovesicular carrier system for ocular delivery. *Int J Pharm*. 2011;413(1–2):202–210. doi:10.1016/j.ijpharm.2011.04.027
12. Basha M, Abd El-Alim SH, Shamma RN, Awad GE. Design and optimization of surfactant-based nanovesicles for ocular delivery of Clotrimazole. *J Liposome Res*. 2013;23(3):203–210. doi:10.3109/08982104.2013.788025
13. Elsherif NI, Shamma RN, Abdelbary G. Terbinafine hydrochloride trans-ungual delivery via nanovesicular systems: in vitro characterization and ex vivo evaluation. *AAPS PharmSciTech*. 2017;18(2):551–562. doi:10.1208/s12249-016-0528-9
14. Farghaly DA, Aboelwafa AA, Hamza MY, Mohamed MI. Topical delivery of fenoprofen calcium via elastic nano-vesicular spanlastics: optimization using experimental design and in vivo evaluation. *AAPS PharmSciTech*. 2017;18(8):2898–2909. doi:10.1208/s12249-017-0771-8
15. Kamboj S, Saini V, Magon N, Bala S, Jhawat V. Vesicular drug delivery systems: a novel approach for drug targeting. *Brain*. 2013;1:11.
16. Sharma N, Bhardwaj V, Singh S, et al. Simultaneous quantification of triterpenoic acids by high performance liquid chromatography method in the extracts of gum resin of Boswellia serrata obtained by different extraction techniques. *Chem Cent J*. 2016;10(1):49. doi:10.1186/s13065-016-0194-8
17. Chevrier MR, Ryan AE, Lee DY-W, Zhongze M, Wu-Yan Z, Via CS. Boswellia carterii extract inhibits TH1 cytokines and promotes TH2 cytokines in vitro. *Clin Diagn Lab Immunol*. 2005;12(5):575–580. doi:10.1128/CDLI.12.5.575-580.2005
18. Jauch J, Bergmann J. An efficient method for the large-scale preparation of 3- O -Acetyl-11-oxo- β - boswellic acid and other boswellic acids. *Eur J Org Chem*. 2003;24:4752–4756. doi:10.1002/ejoc.200300386
19. Singh S, Khajuria A, Taneja C, Khajuria RK, Nabi G. Boswellic acids and glucosamine show synergistic effect in preclinical anti-inflammatory study in rats. *Bioorg Med Chem Lett*. 2007;17:3706–3711. doi:10.1016/j.bmcl.2007.04.034
20. Gohel M, Soni T, Hingorani L, Patel A, Patel N. Development and optimization of plant extract loaded nanoemulsion mixtures for the treatment of inflammatory disorder. *Curr Res Drug Discov*. 2014;1(2):29–38. doi:10.3844/crddsp.2014.29.38
21. Alam MA, Al-Jenoobi FI, Al-Mohizea AM, Ali R. Effervescence assisted fusion technique to enhance the solubility of drugs. *AAPS PharmSciTech*. 2015;16(6):1487–1494. doi:10.1208/s12249-015-0381-2
22. Larsson J Methods for measurement of solubility and dissolution rate of sparingly soluble drugs; 2009.
23. Rohit K. Preliminary test of phytochemical screening of crude ethanolic and aqueous extract of Moringa pterygosperma Gaertn. *J Pharmacogn Phytochem*. 2015;4(1):07–09.
24. Kumar U, Kumar B, Bhandari A, Kumar Y. Phytochemical investigation and comparison of antimicrobial screening of clove and cardamom. *Int J Pharm Sci Res*. 2010;1(12):138–147.
25. Alotaibi S. Biophysical properties and finger print of Boswellia Sp. Burseraceae. *Saudi J Biol Sci*. 2019;26(7):1450–1457. doi:10.1016/j.sjbs.2019.09.019
26. Sailer ER, Subramanian LR, Rall B, Hoernlein RF, Ammon HP, Safayhi H. Acetyl-11-keto-β-boswellic acid (AKBA): structure requirements for binding and 5-lipoxygenase inhibitory activity. *Br J Pharmacol*. 1996;117(4):615–618. doi:10.1111/j.1476-5381.1996.tb15235.x
27. Shah SA, Rathod IS, Suhagia BN, Pandya SS, Parmar VK. A simple high-performance liquid chromatographic method for the estimation of boswellic acids from the market formulations containing Boswellia serrata extract. *J Chromatogr Sci*. 2008;46(8):735–738. doi:10.1093/chromsci/46.8.735
28. Mehta M, Satija S, Garg M. Comparison between HPLC and HPTLC densitometry for the determination of 11-keto-β-boswellic acid and 3-acetyl-11-keto-β-boswellic acid from boswellia serrata extract. *Indian J Pharm Educ Res*. 2016;50(3):418–423. doi:10.5530/ijper.50.3.15
29. Miscioscia E, Shmalberg J, Scott KC. Measurement of 3-acetyl-11-keto-beta-boswellic acid and 11-keto-beta-boswellic acid in boswellia serrata supplements administered to dogs. *BMC Vet Res*. 2019;15(1):270. doi:10.1186/s12917-019-2021-7

30. Mali N, Darandale S, Vavia P. Niosomes as a vesicular carrier for topical administration of minoxidil: formulation and in vitro assessment. *Drug Deliv Transl Res*. 2013;3(6):587–592. doi:10.1007/s13346-012-0083-1
31. Fahmy AM, El-Setouhy DA, Ibrahim AB, Habib BA, Tayel SA, Bayoumi NA. Penetration enhancer-containing spanlastics (PECSs) for transdermal delivery of haloperidol: in vitro characterization, ex vivo permeation and in vivo biodistribution studies. *Drug Deliv*. 2018;25(1):12–22. doi:10.1080/10717544.2017.1410262
32. Jiang J, Ma T, Zhang L, Cheng X, Wang C. The transdermal performance, pharmacokinetics, and anti-inflammatory pharmacodynamics evaluation of harmine-loaded ethosomes. *Drug Dev Ind Pharm*. 2020;46(1):101–108. doi:10.1080/03639045.2019.1706549
33. Manosroi A, Jantrawut P, Manosroi J. Anti-inflammatory activity of gel containing novel elastic niosomes entrapped with diclofenac diethylammonium. *Int J Pharm*. 2008;360(1–2):156–163. doi:10.1016/j.ijpharm.2008.04.033
34. Al-mahallawi AM, Khowessah OM, Shoukri RA. Nano-transfersomal ciprofloxacin loaded vesicles for non-invasive trans-tympanic ototopical delivery: in-vitro optimization, ex-vivo permeation studies, and in-vivo assessment. *Int J Pharm*. 2014;472(1–2):304–314. doi:10.1016/j.ijpharm.2014.06.041
35. Mazyed EA, Abdelaziz AE. Fabrication of transgelosomes for enhancing the ocular delivery of acetazolamide: statistical optimization, in vitro characterization, and in vivo study. *Pharmaceutics*. 2020;12(5):465. doi:10.3390/pharmaceutics12050465
36. El Gamal SS, Naggar VF, Allam AN. Optimization of acyclovir oral tablets based on gastroretention technology: factorial design analysis and physicochemical characterization studies. *Drug Dev Ind Pharm*. 2011;37(7):855–867. doi:10.3109/03639045.2010.546404
37. Finnin B, Walters KA, Franz TJ. In vitro skin permeation methodology. In: Heather AEB, Adam CW, eds. Transdermal and Topical Drug Delivery: Principles and Practice. Hoboken, NJ, USA: John Wiley & Sons; 2012:85-108.
38. Mazyed EA, Zakaria S. Enhancement of dissolution characteristics of clopidogrel bisulphate by proniosomes. *Int J Appl Pharm*. 2019;11(2):77–85. doi:10.22159/ijap.2019v11i2.30575
39. Abd-Elal RM, Shamma RN, Rashed HM, Bendas ER. Trans-nasal zolmitriptan novasomes: in-vitro preparation, optimization and in-vivo evaluation of brain targeting efficiency. *Drug Deliv*. 2016;23(9):3374–3386. doi:10.1080/10717544.2016.1183721
40. Bansal S, Aggarwal G, Chandel P, Harikumar S. Design and development of cefdinir niosomes for oral delivery. *J Pharm Bioallied Sci*. 2013;5(4):318. doi:10.4103/0975-7406.120080
41. Das B, Sen SO, Maji R, Nayak AK, Sen KK. Transferosomal gel for transdermal delivery of risperidone: formulation optimization and ex vivo permeation. *J Drug Deliv Sci Technol*. 2017;38:59–71. doi:10.1016/j.jddst.2017.01.006
42. Gupta A, Prajapati SK, Balamurugan M, Singh M, Bhatia D. Design and development of a proniosomal transdermal drug delivery system for captopril. *Trop J Pharm Res*. 2007;6(2):687–693. doi:10.4314/tjpr.v6i2.14647
43. Moore JW, Flanner HH. Mathematical comparison of curves with an emphasis on in Vitro Dissolution Profiles. *Pharm Technol*. 1996;20(6):64-74.
44. Kilkenny C, Browne WJ, Cuthill IC, Emerson M, Altman DG. Improving bioscience research reporting: the ARRIVE guidelines for reporting animal research. *PLoS Biol*. 2010;8(6):e1000412. doi:10.1371/journal.pbio.1000412
45. Hollands C. The animals (scientific procedures) Act 1986. *Lancet (London, England)*. 1986;2(8497):32. doi:10.1016/S0140-6736(86)92571-7
46. Directive E. 63/EU of the European Parliament and of the Council of 22 September 2010 on the protection of animals used for scientific purposes. *Off J Eur Union*. 2010;276(33):33–79.
47. Mustapha RB, Lafforgue C, Fenina N, Marty J. Influence of drug concentration on the diffusion parameters of caffeine. *Indian J Pharmacol*. 2011;43(2):157. doi:10.4103/0253-7613.77351
48. El Maghraby GM, Ahmed AA, Osman MA. Penetration enhancers in proniosomes as a new strategy for enhanced transdermal drug delivery. *Saudi Pharm J*. 2015;23(1):67–74. doi:10.1016/j.jsps.2014.05.001
49. Jaafar-Maalej C, Diab R, Andrieu V, Elaissari A, Fessi H. Ethanol injection method for hydrophilic and lipophilic drug-loaded liposome preparation. *J Liposome Res*. 2010;20(3):228–243. doi:10.3109/08982100903347923
50. Garg V, Singh H, Bhatia A, et al. Systematic development of transethosomal gel system of piroxicam: formulation optimization, in vitro evaluation, and ex vivo assessment. *AAPS PharmSciTech*. 2017;18(1):58–71. doi:10.1208/s12249-016-0489-z
51. Leonyza A, Surini S. Optimization of sodium deoxycholate-based transfersomes for percutaneous delivery of peptides and proteins. *Int J Appl Pharm*. 2019;329–332. doi:10.22159/ijap.2019v11i5.33615
52. Elazreg R. Formulation and in vitro evaluation of methazolamide elastic vesicular systems. *Al-Azhar J Pharm Sci*. 2014;49(1):75–84. doi:10.21608/ajps.2014.6958
53. Gupta PN, Mishra V, Singh P, et al. Tetanus toxoid-loaded transfersomes for topical immunization. *J Pharm Pharmacol*. 2005;57(3):295–301. doi:10.1211/0022357055515
54. Yassin GE, Amer RI, Fayez AM. Carbamazepine loaded vesicular structures for enhanced brain targeting via intranasal route: optimization, in vitro evaluation, and in vivo study. *Int J Appl Pharm*. 2019;11(4):264–274. doi:10.22159/ijap.2019v11i4.33474
55. Araujo J, Gonzalez-Mira E, Egea M, Garcia M, Souto E. Optimization and physicochemical characterization of a triamcinolone acetonide-loaded NLC for ocular antiangiogenic applications. *Int J Pharm*. 2010;393(1–2):168–176. doi:10.1016/j.ijpharm.2010.03.034
56. Fang J-Y, Yu S-Y, Wu P-C, Huang Y-B, Tsai Y-H. In vitro skin permeation of estradiol from various proniosome formulations. *Int J Pharm*. 2001;215(1–2):91–99. doi:10.1016/S0378-5173(00)00669-4
57. Chauhan M, Malik S. Formulation and optimization of novel elastic nano-vesicular carrier of vancomycin hydrochloride for enhanced corneal permeability. *IJPRS*. 2016;5(4):88–100.
58. Ngan CL, Basri M, Lye FF, et al. Comparison of process parameter optimization using different designs in nanoemulsion-based formulation for transdermal delivery of fullerene. *Int J Nanomedicine*. 2014;9:4375. doi:10.2147/IJN.S65689
59. Li P-H, Chiang B-H. Process optimization and stability of D-limonene-in-water nanoemulsions prepared by ultrasonic emulsification using response surface methodology. *Ultrason Sonochem*. 2012;19(1):192–197. doi:10.1016/j.ultsonch.2011.05.017
60. Andersen T, Vanić Ž, Flaten GE, Mattsson S, Tho I, Škalko-Basnet N. Pectosomes and chitosomes as delivery systems for metronidazole: the one-pot preparation method. *Pharmaceutics*. 2013;5(3):445–456. doi:10.3390/pharmaceutics5030445
61. El Zaafarany GM, Awad GA, Holayel SM, Mortada ND. Role of edge activators and surface charge in developing ultradeformable vesicles with enhanced skin delivery. *Int J Pharm*. 2010;397(1–2):164–172. doi:10.1016/j.ijpharm.2010.06.034
62. Jain S, Jain P, Umamaheshwari R, Jain N. Transfersomes—a novel vesicular carrier for enhanced transdermal delivery: development, characterization, and performance evaluation. *Drug Dev Ind Pharm*. 2003;29(9):1013–1026. doi:10.1081/DDC-120025458
63. Gaur PK, Mishra S, Purohit S. Solid lipid nanoparticles of guggul lipid as drug carrier for transdermal drug delivery. *Biomed Res Int*. 2013;2013:1–10. doi:10.1155/2013/750690

64. Deshkar SS, Sonkamble KG, Mahore JG. Formulation and optimization of nanosuspension for improving solubility and dissolution of gemfibrozil. *Asian J Pharm Clin Res*. 2019;12(1):157–163. doi:10.22159/ajpcr.2019.v12i1.26724
65. Dora CP, Singh SK, Kumar S, Datusalia AK, Deep A. Development and characterization of nanoparticles of glibenclamide by solvent displacement method. *Acta Pol Pharm*. 2010;67(3):283–290.
66. Danaei M, Dehghankhold M, Ataei S, et al. Impact of particle size and polydispersity index on the clinical applications of lipidic nanocarrier systems. *Pharmaceutics*. 2018;10(2):57. doi:10.3390/pharmaceutics10020057
67. Darwhekar G, Jain DK, Choudhary A. Elastic liposomes for delivery of neomycin sulphate in deep skin infection. *Asian J Pharm Sci*. 2012;7:230–240.
68. ElMeshad AN, Mohsen AM. Enhanced corneal permeation and antimycotic activity of itraconazole against Candida albicans via a novel nanosystem vesicle. *Drug Deliv*. 2016;23(7):2115–2123. doi:10.3109/10717544.2014.942811
69. Basalious EB, Shawky N, Badr-Eldin SM. SNEDDS containing bioenhancers for improvement of dissolution and oral absorption of lacidipine. I: development and optimization. *Int J Pharm*. 2010;391(1–2):203–211. doi:10.1016/j.ijpharm.2010.03.008
70. Kazi KM, Mandal AS, Biswas N, et al. Niosome: a future of targeted drug delivery systems. *J Adv Pharm Technol Res*. 2010;1(4):374. doi:10.4103/0110-5558.76435
71. Das MK, Palei NN. Sorbitan ester niosomes for topical delivery of rofecoxib. *Indian J Exp Biol*. 2011;49:438–445.
72. Sengodan T, Sunil B, Vaishali R, Chandra RJ, Nagar S, Nagar O. Formulation and evaluation of maltodextrin based proniosomes loaded with indomethacin. *Int J PharmTech Res*. 2009;1(3):517–523.
73. Ren W, Tian G, Jian S, et al. TWEEN coated NaYF 4: yb, Er/NaYF4 core/shell upconversion nanoparticles for bioimaging and drug delivery. *RSC Adv*. 2012;2(18):7037–7041. doi:10.1039/c2ra20855e
74. El-Sayed MM, Hussein AK, Sarhan HA, Mansour HF. Flurbiprofen-loaded niosomes-in-gel system improves the ocular bioavailability of flurbiprofen in the aqueous humor. *Drug Dev Ind Pharm*. 2017;43(6):902–910. doi:10.1080/03639045.2016.1272120
75. Fathalla D, Youssef EM, Soliman GM. Liposomal and ethosomal gels for the topical delivery of anthralin: preparation, comparative evaluation and clinical assessment in psoriatic patients. *Pharmaceutics*. 2020;12(5):446. doi:10.3390/pharmaceutics12050446
76. Bairwa K, Jachak SM. Development and optimisation of 3-Acetyl-11-keto-β-boswellic acid loaded poly-lactic-co-glycolic acid-nanoparticles with enhanced oral bioavailability and in-vivo anti-inflammatory activity in rats. *J Pharm Pharmacol*. 2015;67(9):1188–1197. doi:10.1111/jphp.12420
77. Fang J-Y, Fang C-L, Liu C-H, Su Y-H. Lipid nanoparticles as vehicles for topical psoralen delivery: solid lipid nanoparticles (SLN) versus nanostructured lipid carriers (NLC). *Eur J Pharm Biopharm*. 2008;70(2):633–640. doi:10.1016/j.ejpb.2008.05.008
78. Pramod K, Suneesh CV, Shanavas S, Ansari SH, Ali J. Unveiling the compatibility of eugenol with formulation excipients by systematic drug-excipient compatibility studies. *J Anal Sci Technol*. 2015;6(1):34. doi:10.1186/s40543-015-0073-2
79. Rahman SA, Abdelmalak NS, Badawi A, Elbayoumy T, Sabry N, Ramly AE. Formulation of tretinoin-loaded topical proniosomes for treatment of acne: in-vitro characterization, skin irritation test and comparative clinical study. *Drug Deliv*. 2015;22(6):731–739. doi:10.3109/10717544.2014.896428
80. Kakkar S, Pal Kaur I. A novel nanovesicular carrier system to deliver drug topically. *Pharm Dev Technol*. 2013;18(3):673–685. doi:10.3109/10837450.2012.685655
81. Salama HA, Mahmoud AA, Kamel AO, Abdel Hady M, Awad GA. Brain delivery of olanzapine by intranasal administration of transfersomal vesicles. *J Liposome Res*. 2012;22(4):336–345. doi:10.3109/08982104.2012.700460
82. Brodin B, Steffansen B, Nielsen CU. Passive diffusion of drug substances: the concepts of flux and permeability. *Mol Biopharm*. 2010;135–152.